AD-A053 920 LOCKHEED MISSILES AND SPACE CO INC PALO ALTO CALIF PA--ETC F/G 4/1
LOW-ENERGY PARTICLE EXPERIMENT.(U)
MAR 77 E G SHELLEY N00014-72-C-0234
UNCLASSIFIED LMSC/D623448 NL

1 OF 1
AD A053920

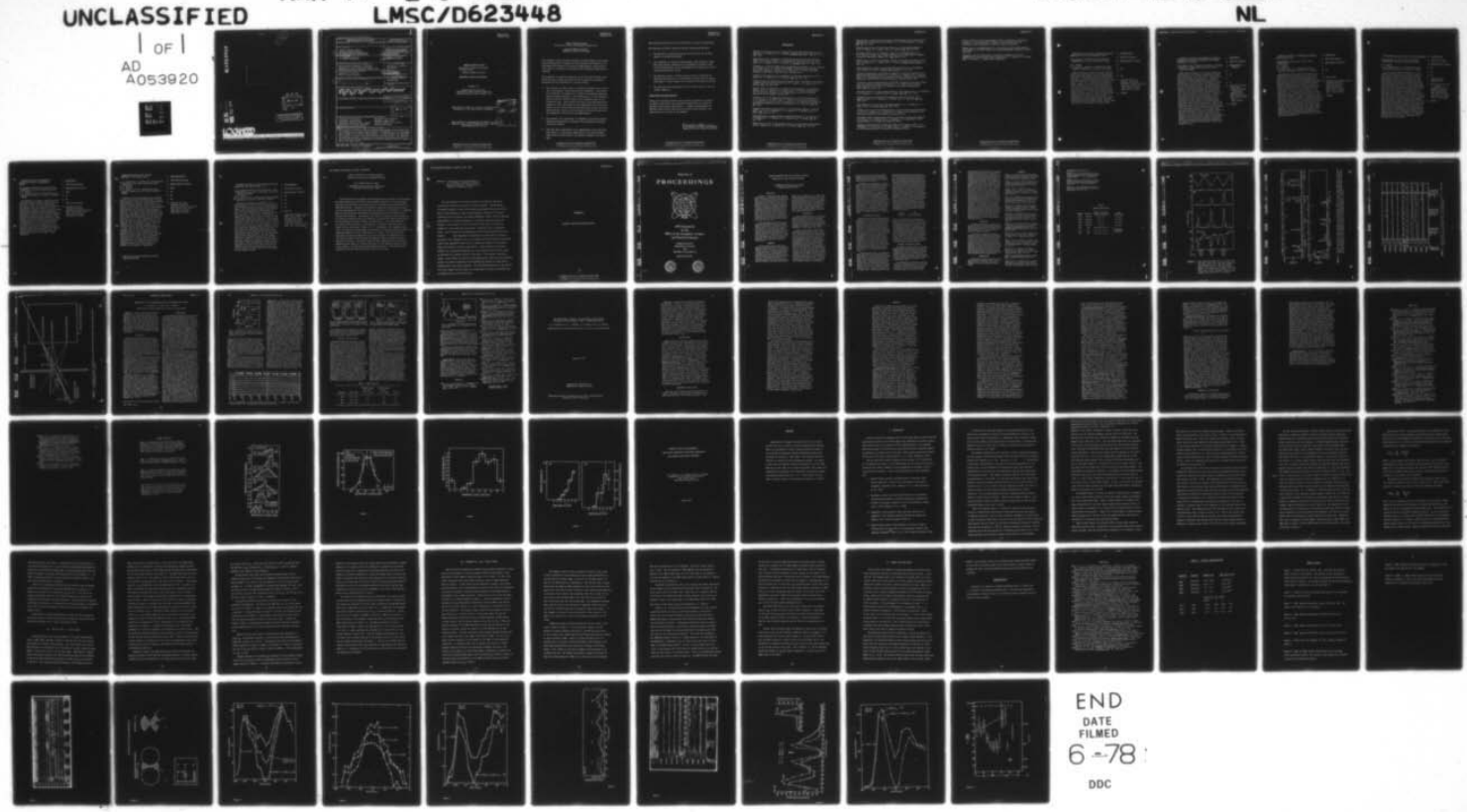

END
DATE FILMED
6-78
DDC

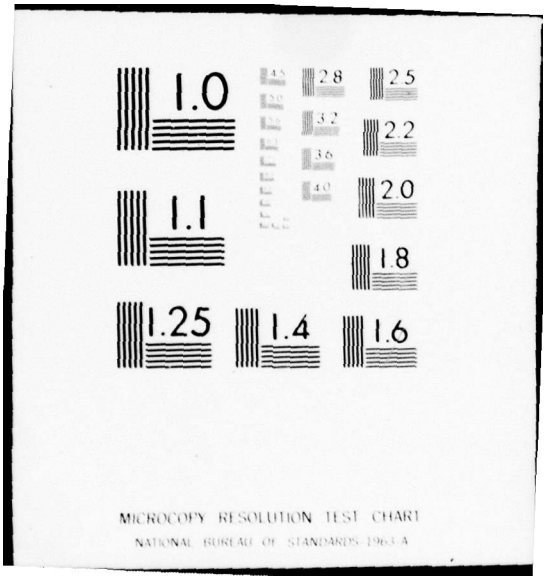
1.0
1.1
1.25
1.4
1.6
1.8
2.0
2.2
2.5
2.8
3.2
3.6
4.0
4.5
5.0
MICROCOPY RESOLUTION TEST CHART
NATIONAL BUREAU OF STANDARDS 1963-A

AD A053920

AD No. ____
DDC FILE COPY

DDC
RECEIVED
MAY 12 1978
A

DISTRIBUTION STATEMENT A
Approved for public release;
Distribution Unlimited

LOCKHEED
MISSILES & SPACE COMPANY, INC. • SUNNYVALE, CALIFORNIA
A SUBSIDIARY OF LOCKHEED AIRCRAFT CORPORATION

SECURITY CLASSIFICATION OF THIS PAGE (When Data Entered)

REPORT DOCUMENTATION PAGE

READ INSTRUCTIONS BEFORE COMPLETING FORM

1. REPORT NUMBER

2. GOVT ACCESSION NO.

3. RECIPIENT'S CATALOG NUMBER

4. TITLE (and Subtitle)

Annual Technical Report
Contract N00014-72-C-0234
Low-Energy Particle Experiment.

5. TYPE OF REPORT & PERIOD COVERED

Annual Technical Report
~~4/1/76 through 3/31/77~~

6. PERFORMING ORG. REPORT NUMBER

LMSC/D623448

7. AUTHOR(s)

Dr. Edward G. Shelley

8. CONTRACT OR GRANT NUMBER(s)

N00014-72-C-0234

9. PERFORMING ORGANIZATION NAME AND ADDRESS

Space Sciences Laboratory (52-12/205)
Lockheed Palo Alto Research Laboratory
3251 Hanover Street, Palo Alto, Calif. 94304

10. PROGRAM ELEMENT, PROJECT, TASK AREA & WORK UNIT NUMBERS

ONR Contract Authority
NR 323-014

11. CONTROLLING OFFICE NAME AND ADDRESS

Department of the Navy
Office of Naval Research

12. REPORT DATE

30 March 1977

13. NUMBER OF PAGES

6

14. MONITORING AGENCY NAME & ADDRESS (if different from Controlling Office)

Annual Technical rept.
1 Apr 77 - 31 Mar 78

15. SECURITY CLASS. (of this report)

UNCLASSIFIED

15a. DECLASSIFICATION/DOWNGRADING SCHEDULE

16. DISTRIBUTION STATEMENT (of this Report)

This document may be further distributed by any holder only with specific prior approval of the Department of the Navy, Office of Naval Research, Arlington, Virginia 22217.

DISTRIBUTION STATEMENT A
Approved for public release;
Distribution Unlimited

17. DISTRIBUTION STATEMENT (of the abstract entered in Block 20, if different from Report)

DDC
RECEIVED
MAY 12 1978
A

18. SUPPLEMENTARY NOTES

19. KEY WORDS (Continue on reverse side if necessary and identify by block number)

low-energy (keV) plasmas
ionospheric perturbations
ionospheric-magnetospheric coupling
magnetospheric plasma composition
low-energy plasma spectrometer
S3-3 (STP 74-2) satellite
energetic oxygen ions
OV1-18 and STP 71-2 satellites
modified instrument

20. ABSTRACT (Continue on reverse side if necessary and identify by block number)

This program is directed toward an improved understanding of the sources and the energization, transport and loss processes associated with the low-energy (keV) plasmas in the earth's magnetosphere. A low-energy particle experiment was launched on the Air Force S3-3 satellite in July of 1976. The experiment is operating completely successfully and has made several major discoveries about previously unknown ionospheric acceleration mechanisms and the composition of the ring current.

DD FORM 1 JAN 73 1473 EDITION OF 1 NOV 65 IS OBSOLETE

210 118

UNCLASSIFIED

SECURITY CLASSIFICATION OF THIS PAGE (When Data Entered)

LMSC/D623448
31 March 1978

ANNUAL TECHNICAL REPORT

(For period 1 April 1977 through
31 March 1978)

Contract N00014-72-C-0234

See A039763

LOW-ENERGY PARTICLE EXPERIMENT

Prepared by

Space Sciences Laboratory
Lockheed Palo Alto Research Laboratory
Lockheed Missiles & Space Company, Inc.

ACCESSION for
NTIS White Section
DDC Buff Section
UNANNOUNCED
JUSTIFICATION
Letter on file
BY
DISTRIBUTION/AVAILABILITY CODES
Dist. AVAIL. and/or SPECIAL
A

Reproduction in whole or in part is permitted for any purpose of the United States Government.

This research was sponsored by the Office of Naval Research under Contract N00014-72-C-0234, ONR Contract Authority NR 323-014.

LOCKHEED PALO ALTO RESEARCH LABORATORY
LOCKHEED MISSILES & SPACE COMPANY, INC.
A SUBSIDIARY OF LOCKHEED AIRCRAFT CORPORATION

ANNUAL TECHNICAL REPORT
(For period 1 April 1976 through 31 March 1977)

Contract N00014-72-C-0234
LOW-ENERGY PARTICLE EXPERIMENT

This program is directed toward an improved understanding of the sources and the energization, transport and loss processes associated with the low-energy (keV) plasmas in the earth's magnetosphere, particularly as they relate to ionospheric perturbations and ionospheric-magnetospheric coupling.

The experiment is operating completely successfully and has made three major discoveries about previously unknown ionospheric acceleration mechanisms and the composition of the ring current.

1. The discovery of large fluxes of energized ionospheric ions streaming up the magnetic field lines from the ionosphere. This discovery establishes the existence of a major new ionospheric-magnetospheric coupling phenomenon. The characteristics of the phenomenon point to parallel electric fields as the immediate cause of the accelerated ions. These results and those of the ONR companion experiment on S3-3, which makes in situ measurements of the electric fields, put on a firm basis the many recent speculations and inferences relating to large electric potential differences parallel to the geomagnetic field lines in the magnetosphere.

2. The discovery of a second type of ionospheric acceleration mechanism which preferentially accelerates the perpendicular component of the ion velocity.

3. The first direct measurement of the composition of the storm-time ring current. In the energy range from 1-16 keV the main phase ring current has been found to be primarily composed of H^+ and O^+ ions.

More detailed discussions of the results will be found in the appendix.

Our principal activities during the present reporting period were:

1. The provision of technical planning and liaison for the on-orbit support of the ONR-118 payload.

2. The performance of surveys of approximately 1000 additional flight data tapes and the conducting of a preliminary statistical study on the characteristics of the upstreaming field alligned ion events observed during these surveys.

3. The detailed analysis of three events in order to establish the principal characteristics of the parallel electric field structures which appear to play a major role in auroral acceleration processes.

4. The publication and presentation of the initial results to the scientific community.

Publications and Presentations

During this reporting period we have prepared, published or presented 4 invited review papers; 14 contributed presentations at scientific meetings; and 4 written publications. A complete bibliography of the ONR-118 results follows and copies of the most recent abstracts and publications are included in the appendix.

E. G. Shelley

E. G. Shelley, Principal Investigator
Lockheed Palo Alto Research Laboratory

Bibliography

"Satellite Observations of an Ionospheric Acceleration Mechanism," by E. G. Shelley, R. D. Sharp, and R. G. Johnson, Geophys. Res. Lett., Vol. 3, No. 11, 654, 1976.

"Observation of an Ionospheric Acceleration Mechanism Producing Energetic (keV) Ions Primarily Normal to the Geomagnetic Field Direction," by R. D. Sharp, R. G. Johnson, and E. G. Shelley, J. Geophys. Res., 82, 3324, 1977.

"Composition of the Hot Plasma Near Geosynchronous Altitude, by R. G. Johnson, R. D. Sharp, and E. G. Shelley, Proceedings of the Spacecraft Charging Technology Conference, edited by C. P. Pike and R. R. Lovell, Air Force Geophysical Laboratory, AFGL-TR-770051, February 1977.

"Satellite Observations of an Ionospheric Acceleration Mechanism," by E. G. Shelley, R. D. Sharp, and R. G. Johnson, EOS, 57, 992, 1976.

"Characteristics of Upward-Flowing, Energetic (keV), Ionospheric Ions During a Magnetically-Disturbed Period," by R. G. Johnson, R. D. Sharp, and E. G. Shelley, EOS, 57, 993, 1976.

"Recent Results of Energetic Ion Composition Measurements in the Magnetosphere," by R. D. Sharp, R. G. Johnson, and E. G. Shelley, presented at the International Symposium on the Magnetosphere and Its Environment, Christchurch, New Zealand, January 1977.

"Energetic (keV) Ion Composition Observations on the S3-3 Satellite," by R. G. Johnson, R. D. Sharp, and E. G. Shelley, invited paper presented at the special session on the S3-3 satellite at the Spring 1977 meeting of the American Geophysical Union in Washington, D. C., May 1977, EOS, 58, 991, 1977.

"Angular Distribution Characteristics of Up-Streaming Energetic (keV) O^+ and H^+ Ions," by A. Ghielmetti, R. G. Johnson, E. G. Shelley, and R. D. Sharp, EOS, 58, 473, 1977.

"The Morphology of Upward-Flowing Field-Aligned Energetic Ion Fluxes," by A. Ghielmetti, E. G. Shelley, R. G. Johnson, and R. D. Sharp, EOS, 58, 716, 1977.

"Observation of Ions of Ionospheric Origin in the Storm-Time Ring Current," by R. G. Johnson, R. D. Sharp, and E. G. Shelley, EOS, 58, 753, 1977.

"Distribution of Electrostatic Potential Along Magnetic Field Inferred from Observations of Electron and Ion Fluxes," by J. B. Cladis and R. D. Sharp, EOS, 58, 716, 1977.

"Observations of Ions of Solar Wind Origin in the Inner Magnetosphere," by E. G. Shelley, R. D. Sharp, and R. G. Johnson, EOS, 58, 716, 1977.

"Energetic Heavy Ions of Ionospheric Origin in the Magnetosphere," by E. G. Shelley, invited review paper presented at the IAGA General Assembly in Seattle, Washington, August 1977, EOS, 58 752, 1977.

"Observations of Ions of Ionospheric Origin in the Storm Time Ring Current," by R. G. Johnson, R. D. Sharp, and E. G. Shelley, Geophys. Res. Letters, 4, 403, 1977.

"The Latitudinal, Diurnal, and Altitudinal Distributions of Up-Streaming Field Aligned Ion Fluxes, Geophys. Res. Letters, 5, 59, 1978.

"Satellite Measurements from Within Ionospheric Structures Responsible for Auroral Acceleration Processes," R. D. Sharp, E. G. Shelley, R. G. Johnson, Paper 2-12, Proceedings of the Ionospheric Effects Symposium, Naval Research Laboratory, and the Office of Naval Research, January 24-26, 1978.

"A Review of Particle Measurements from Within Ionospheric Structures Responsible for Auroral Acceleration Processes," R. D. Sharp invited review paper presented at the Fall, 1977 meeting of the American Geophysical Union, EOS, 58, 1209, 1977.

"Average Properties of Upstreaming Energetic Field Aligned Ions," A. Ghielmetti, R. G. Johnson, E. G. Shelley, and R. D. Sharp, EOS, 58, 1211, 1977.

"Observations of the Ring Current Composition During the 29 July 1977 Magnetic Storm," R. G. Johnson, R. D. Sharp, and E. G. Shelley, EOS, 58, 1217, 1977.

"Ion Composition of the Quiet Time Magnetosphere," E. G. Shelley, R. D. Sharp, and R. G. Johnson, EOS, 58, 1217, 1977.

"Evidence for Ions of Solar Wind Origin in the Storm Time Ring Current Near L = 4," R. G. Johnson, E. G. Shelley, R. D. Sharp, to be presented at the 1978 Spring Meeting of the American Geophysical Union.

"Energetic Particle Measurements Within an Inverted V Acceleration Region," R. D. Sharp, E. G. Shelley, and R. G. Johnson, to be presented at 1978 Spring Meeting of the American Geophysical Union.

"Downward Streaming Field Aligned Ion Fluxes in the Auroral Zone," A. G. Ghielmetti, E. G. Shelley, R. D. Sharp, and R. G. Johnson, to be presented at 1978 Spring Meeting of the American Geophysical Union.

"Scale of Electric Field Along Magnetic Field in Structures of Inverted V Events," J. B. Cladis and R. D. Sharp, to be presented at Solar Terrestrial Physics Symposium, Innsbruck, Austria, June 1978.

"Heavy Ions in the Magnetosphere," E. G. Shelley, invited review paper to be presented at the Solar Terrestrial Physics Symposium, Innsbruck, Austria, June 1978.

"Energetic Particle Measurements from Within Ionospheric Structures Responsible for Auroral Acceleration Processes," R. D. Sharp, R. G. Johnson, and E. G. Shelley, J. Geophys. Res. (Submitted).

OBSERVATIONS OF THE RING CURRENT COMPOSITION DURING THE 29 JULY 1977 MAGNETIC STORM

R. G. Johnson (Lockheed Palo Alto Research Laboratory, Palo Alto, California 94304)

R. D. Sharp
E. G. Shelley (both at: Lockheed Palo Alto Research Laboratory, Palo Alto, Ca. 94304)

Data on the ring current composition during the 29 July 1977 magnetic storm were acquired near apogee (8000 km) of the S3-3 (1976-065B) satellite. The measurements were made with an ion mass spectrometer covering the energy range from 0.5 to 16 keV. During the main phase ($D_{st} \hat{} = 100\gamma$) of the storm, the ratio of O^+/H^+ number densities in the inner ring current ($L < 4$) is significantly higher than observed in three previous storms with comparable peak values of D_{st}. He^+ fluxes were also observed during the main phase but the intensities were small compared to the O^+ and H^+ fluxes. A comparison of the results from the main phase of the 29 July 1977 magnetic storm with the results from the 29 December 1976, 6 April 1977, and 19 April 1977 magnetic storms is made.

1. 003186JOHNSON
2. 1977 Fall Meeting
3. Magnetospheric Physics
4.
5. No
6.
7. 0%
8. Lockheed Palo Alto Research Laboratory Technical Information Center Dept. 52-52, Bldg. 201 3251 Hanover Street Palo Alto, Ca. 94304
9. 301808

A REVIEW OF PARTICLE MEASUREMENTS FROM WITHIN IONOSPHERIC STRUCTURES RESPONSIBLE FOR AURORAL ACCELERATION PROCESSES

R. D. Sharp (Space Sciences Laboratory, Lockheed Palo Alto Research Laboratory, Palo Alto, California 94304)

Large scale ionospheric structures containing field aligned d.c. electric fields are thought to be responsible for "inverted V" events and at least some types of auroral arcs. Because of its unique orbital characteristics, the S3-3 satellite is for the first time making measurements within these structures at altitudes of $\approx$ 1 RE in the polar regions. Particle measurements by the Aerospace group with electrosatic analyzers and by the Lockheed group with energetic ion mass spectrometers and magnetic electron spectrometers will be reviewed. Details of the energy and angular distributions of the electrons and ions in the keV range allow inferences to be made about the geometry of the structures and the nature of the acceleration processes taking place within them. Some of the characteristics of the structures are similar to those which have been predicted for the "inverted V" acceleration regions. In two events which have been analyzed in detail a vertical extent of the parallel electric field of $\geq 10^3$km is inferred. An event on 29 July 1976 in which the Berkeley group has reported intense electrostatic shocks will be described utilizing the results of both the Aerospace and Lockheed experiments. The energy of the accelerated ions in this event exceeded 16 keV.

1. 002641SHARP
2. 1977 Fall Meeting
3. Magnetospheric Physics
4.
5. No
6.
7. O
8. Technical Information Center
Lockheed Research Laboratory
D/5250, B/201
3251 Hanover St.
Palo Alto, Ca.94304
Attn:
Judy Conahan
9. 301808

AVERAGE PROPERTIES OF UPSTREAMING ENERGETIC FIELD ALIGNED IONS

A. Ghielmetti (University of Bern, Bern, Switzerland
R. G. Johnson
E. G. Shelley
R. D. Sharp (all at: Lockheed Palo Alto Research Laboratory, Palo Alto, Ca. 94304)

Magnetically field aligned ion fluxes have been observed to stream out of the polar ionosphere in a region closely associated with the auroral oval. The maximum probability of occurrence as observed by the Lockheed energetic ion-spectrometer on the S3-3 satellite (1976-065B) is approximately 35% within a single invariant latitude-magnetic local time-altitude element of size 2° by 3 hrs by 1000 km. The frequency of occurrence distribution has been compared to the frequency of occurrence of overhead aurora near local midnight during the IQSY and good agreement is found. A dawn-dusk asymmetry both in the frequency of occurrence and in the energy distribution is inferred from the data. Fluxes are generally hardest at dusk, with the O^+ ions being more energetic than the H^+ ions. Initial results indicate that the fluxes become harder during magnetic storms and toward local midnight. From the altitude distribution we conclude that the primary acceleration zone is most frequently situated above 6000 km and often extends above 8000 km.

1. 002641SHARP
2. 1977 Fall Meeting
3. Magnetospheric Physics
4.
5. No
6.
7. 30% at IAGA
8. Technical Information Center
   Lockheed Palo Alto
   Research Laboratory
   Dept. 52-50,B/201
   3251 Hanover Street
   Palo Alto, Ca. 94304
   Attn: Judy Conahan
9. 301808

ION COMPOSITION IN THE QUIET TIME MAGNETOSPHERE

E. G. Shelley (Lockheed Palo Alto Research Laboratory, Palo Alto, California 94304)

R. D. Sharp
R. G. Johnson (both at: Lockheed Palo Alto Research Laboratory, Palo Alto, Ca. 94304)

Data on the hot plasma composition in the earth's magnetopshere in the energy range 0.5 to 16 keV is being acquired with an ion mass spectrometer aboard the 1976-065B satellite. The satellite is in an 82° inclination orbit, with perigee near 260 km and apogee near 8060 km, and is spinning such that pitch angle data are obtained for the ions. The ion composition during selected magnetically quiet-time periods has been investigated in the regions of the quiet time ring current and plasma sheet at altitudes below 8000 km in the midnight sector. He^{++} ions were observed in several passes and in one case they were found as low as L = 5.5 which was near the low latitude edge of the plasma sheet electrons. These observations of He^{++} in the absence significant fluxes of He^{+} show that solar wind ions are entering the magnetosphere and are being transported to relatively low L-shells in the magnetosphere during magnetically quiet times. In the energy per nucleon range from 0.5 keV/AMU to 8 keV/AMU the average phase density ratio between He^{++} and H^{+} was found to lie in the 3% to 5% range, consistent with average solar wind ratios.

1. 071063SHELLEY
2. 1977 Fall Meeting
3. Magnetospheric Physics
4. No
5. No
6. No
7. 30% IAGA/IAMAP
   Seattle 1977
8. Technical Information Center
   Lockheed Palo Alto Research Laboratory
   Dept. 52-50,B/201
   3251 Hanover Street
   Palo Alto, Ca. 94304
   Attn: Judy Conahan
9. 301808

ENERGETIC PARTICLE MEASUREMENTS WITHIN AN INVERTED V ACCELERATION REGION

R. D. Sharp (Lockheed Palo Alto Research Laboratory, Palo Alto, California 94304
E. G. Shelley
R. G. Johnson (both at: Lockheed Palo Alto Research Laboratory, Palo Alto, California 94304)

On September 15, 1976 at 1058 UT the S3-3 satellite passed through a single isolated inverted-V region of about two degrees latitudinal width at an altitude of 7000 km and centered near 74° invariant latitude The measured energetic electron and ion fluxes within the structure showed a remarkable latitudinal symmetry which indicates temporal stability in this case. The electron pitch-angle distributions showed evidence of field aligned electric fields both above and below the satellite with a total potential drop of approximately 2 kV. A plausible interpretation of the data suggests that the vertical extent of the acceleration region above the satellite was greater than 1000 km in the central portion of the event, and significantly less at the edges of the structure.

1. 002641SHARP
2. 1978 Spring Meeting
3. Magnetospheric Physics
4. None
5. No
6. No
7. 10% at Fall Meeting
8. Lockheed Palo Alto
   Research Laboratory
   Technical Information Center
   Dept. 52-52, Bldg. 201
   3251 Hanover Street
   Palo Alto, CA. 94304

DOWNWARD STREAMING FIELD ALIGNED ION FLUXES IN THE AURORAL ZONE

A. G. Ghielmetti*, (Lockheed Palo Alto Research Laboratory, Palo Alto, California 94304
E. G. Shelley
R. D. Sharp
R. G. Johnson (all at: Lockheed Palo Alto Research Laboratory, Palo Alto, California 94304)

A survey of mass spectrometer data obtained on the S3-3 satellite (1976-65B) has revealed the occasional existence of downward streaming field aligned ion fluxes. These events are seen in the same general regions where upward flowing field aligned and conical distributions are observed but occur much less frequently ($\lesssim$1%) at flux levels above ~2×10^6 keV/cm^2 sec ster keV. The angular and energy distributions have been analyzed in detail in one particular case, where the maximum flux in the downward direction was ~ 5×10^7 protons/cm^2 sec ster keV. We find that these fluxes occur in conjunction with an enhanced flux of non-field aligned ions of comparable energy. Both components have a peaked energy-spectrum of ~ 1 keV. The average ratio of downcoming to trapped flux is ~ 5. The presence of the anti-loss cone in the ~ 10 keV electrons indicates closed field lines. Upward flowing field aligned H^+ and O^+ ions are observed poleward of this region. The observations are suggestive of a conjugate hemisphere origin of both the downward flowing field aligned component and the trapped component in the region of enhancement.

* Visiting scientist University of Bern, Bern, Switzerland

1. 046313GHIELMETTI
2. 1978 Spring Meeting
3. Magnetospheric Physics
4. None
5. No
6. No
7. 0%
8. Lockheed Palo Alto Research Laboratory
   Technical Information Center
   Dept. 52-52, Bldg. 201
   3251 Hanover Street
   Palo Alto, CA. 94304

EVIDENCE FOR IONS OF SOLAR WIND ORIGIN IN THE STORM-TIME RING CURRENT NEAR L = 4

R. G. Johnson (Space Sciences Laboratory, Lockheed Palo Alto Research Laboratory, Palo Alto, California 94304)
E. G. Shelley
R. D. Sharp (both at Lockheed Palo Alto Research Laboratory, Palo Alto, California 94304)

Ion mass spectrometer measurements in the energy range 0.5 to 16 keV were obtained on the S3-3 satellite during the 29 July 1977 magnetic storm. The first apogee (7900 km) pass during the storm was acquired near 0400 hours U.T. (D_{st} = - 24γ) during the ring current build up to a peak D_{st} = -1000γ (U.T. = 0700 hours). During this pass, ring current fluxes of H^+ and O^+ ions were observed as low as L = 3.2 at magnetic local times near 0500 hours. He^{++} fluxes along with other ion fluxes were observed in the region L = 4.0 to 8.6. In the region L = 4.0 to 4.5, H^+ and O^+ were the dominant fluxes with the He^{++} flux being comparable to the He^+ flux. In this region the He^{++} phase space density was about 2% of the H^+ phase space density in the overlapping velocity range. This is compatible with a solar wind origin for the He^{++} ions, whereas the comparable fluxes of He^+ and He^{++} ions and a relatively high He^{++}/H^+ flux ratio is evidence against an ionospheric origin for the He^{++} ions. These observations provide direct evidence that ions of both solar wind and ionospheric origin are contributing to the ring current during the early part of the main phase of this magnetic storm.

1. 003186JOHNSON
2. 1978 Spring Meeting
3. Magnetospheric Physics
4. No
5. No
6. No
7. 0%
8. Bill to:

Technical Information Cent
Dept. 52/50, Bldg. 201
Lockheed Palo Alto
Research Laboratory
3251 Hanover Street
Palo Alto, California 9430
Attn: Ms. Judy Conahan

STP SYMPOSIUM-INNSBRUCK, AUSTRIA JUNE,1978.

Scale of Electric Field Along Magnetic Field in Structures of Inverted-V Events

J.B. Cladis and R.D. Sharp

Lockheed Palo Alto Research Laboratory
Palo Alto, California 94304

The distributions of magnetic-field-aligned electric fields in the structures of several inverted-V events have been examined using data on the pitch-angle and energy distributions of electrons and ions obtained with the polar-orbiting 1976-65B satellite. Generally, electrostatic potential differences are found to occur simultaneously above and below the altitude of the satellite ($\sim$ 6000 km). Both of these potential differences were determined from an analysis of the electron distributions. The analysis also yields the magnetic field intensity, B_1, above the satellite where the potential is zero and the energy distribution of the downgoing electrons (assumed isotropic) at B_1. The total potentials are found to have inverted-V distributions in latitude, with peak values of several kV and latitudinal widths of $\sim 1^{\circ}$. According to the computed values of B_1, the potentials extend above the satellite to distances exceeding 1000 km indicating apparent electric-field values of $\sim$1 mV/m. The electric-field distributions above the spacecraft were also estimated by computing the ion and electron number densities along the magnetic field and using the quasi-neutrality condition. The number densities were computed using the observed upward-directed fluxes of ions and electrons and the downward electron fluxes at B_1 inferred from the electron-distribution analysis. The resulting self-consistent electric fields were also found to be $\sim$ 1 mV/m.

STP SYMPOSIUM-INNSBRUCK, AUSTRIA, JUNE 1978

Abstract: Heavy Ions in the Magnetosphere by
E. G. Shelley, Lockheed Palo Alto
Research Laboratory, 3251 Hanover St.
Palo Alto, California 94304

For the purposes of this review heavy ions include all species of ions having a mass per unit charge of 2 AMU or greater. The discussion is limited primarily to ions in the energy range between 100 eV and 100 keV. Prior to the discovery in 1972 of large fluxes of energetic O^+ ions precipitating into the auroral zone during geomagnetic storms, the only reported magnetospheric ion species observed in this energy range were helium and hydrogen. More recently O^+ and He^+ have been identified as significant components of the storm time ring current, suggesting that an ionospheric source may be involved in the generation of the fluxes responsible for this current. Mass spectrometer measurements on board the S3-3 satellite have shown that ionospheric ions in the auroral zone are frequently accelerated upward along geomagnetic field lines to several keV energy in the altitude region from 5000 km to greater than 8000 km. These observations also show evidence for acceleration perpendicular to the magnetic field and thus cannot be explained by a parallel electric field alone. This auroral acceleration region is most likely the source for the magnetospheric heavy ions of ionospheric origin, but further acceleration would probably be required to brimg them to characteristic ring current energies. S3-3 and GEOS observations of the He^{++}/H^+ ion ratios suggest that the quiet time plasma sheet and outer ring current may be predominately of solar wind origin.

Appendix A

RELEVANT PUBLICATIONS/PRESENTATIONS

Preprints of

PROCEEDINGS

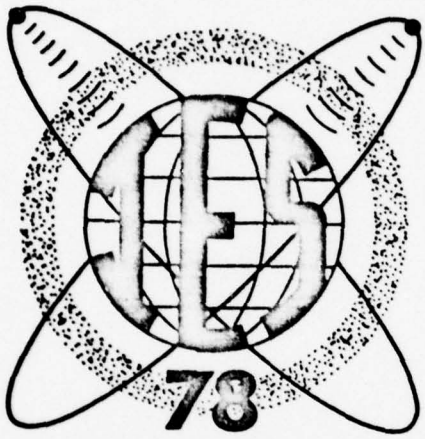

1978 Symposium on the Effect of the Ionosphere on Space and Terrestrial Systems

Jointly Sponsored by
Naval Research Laboratory
and
The Office of Naval Research

January 24-26 1978

SATELLITE MEASUREMENTS FROM WITHIN IONOSPHERIC STRUCTURES RESPONSIBLE FOR AURORAL ACCELERATION PROCESSES

R. D. Sharp, E. G. Shelley, and R. G. Johnson
Lockheed Palo Alto Research Laboratory
Palo Alto, California 94304

INTRODUCTION

Ionospheric disturbances at high latitudes associated with auroral precipitation events are known to cause radio frequency interference problems and so the physical causes of these disturbances are of direct relevance to the theme of this symposium. One class of auroral electron precipitations known as "inverted V" events are thought to be caused by large-scale ionospheric structures containing dc electric fields, with a component parallel to the geomagnetic field resulting in the downward acceleration of the precipitating electrons (Gurnett, 1972; Swift, 1975). Until recently, no direct measurements within these structures have been reported although some of the properties of the auroral acceleration process have been inferred from the characteristics of the precipitating electrons (see review by Evans, 1976).

Recent measurements from within the structures have been acquired by means of directed barium jets (Haerendel, 1976) and from the S3-3 satellite which, because of its unique orbital characteristics, is traversing the structures at altitudes of $\sim 1\ R_E$ in the polar regions. Office of Naval Research experiments on the S3-3 satellite are measuring the characteristics of both the particles and fields within the structures (Shelley et al., 1976; Mozer et al., 1977) and in association with the other spacecraft experiments (Mizera and Fennel, 1977) are providing the first detailed determinations of their geometry.

EXPERIMENT

The S3-3 satellite was launched into an elliptical polar orbit with an initial apogee of 8050 km and perigee of 260 km. The orbital inclination is 97.5°. The satellite is spinning at about 3 rpm with its spin axis perpendicular to the orbital plane. The measurements to be described in this report were acquired from an ion and electron spectrometer experiment mounted with its view direction perpendicular to the spin axis. The experiment consists of 3 ion mass spectrometers and 4 electron spectrometers similar in design to those described previously (Shelley et al., 1972; Reed et al., 1969). The energy ranges and geometric factors of the electron spectrometers are listed in Table 1. The ion mass spectrometers each acquire a 30-channel mass-per-unit-charge spectrum at a single energy-per-unit-charge every second. The energy-per-unit-charge setting is cycled through 4 values every 64 seconds, remaining on each step for 16 seconds. Thus, a 12-point energy spectrum is acquired from the 3 spectrometers every 64 seconds. These 12 measured energy-per-charge values are also listed in Table 1.

OBSERVATIONS

Initial observations from the S3-3 ion mass spectrometer experiment showed intense beams of upward-directed newly-accelerated ionospheric ions as a persistent feature of auroral field lines at altitudes of about 1 RE. Two distinct classes of ion acceleration phenomena have been detected, one involving the parallel and one the perpendicular component of the ion velocity (Shelley et al., 1976; Sharp et al., 1977).

Figure 1 shows a segment of data from the low-energy mass spectrometer acquired in the northern polar region at a local time of about 1430. The relative responses of the O^+ and H^+ ions are plotted versus time and can be compared with the pitch angle determined from the on-board magnetometer shown in the upper panel. The energy-per-unit-charge of the measured ions is also indicated. One sees sharply peaked pitch-angle distributions for both O^+ and H^+ corresponding to ions streaming up the field lines from the ionosphere. The lower panel shows the electron fluxes from the CMEB detector ($0.35 \leq E \leq 1.1$ keV). The deep minima corresponding to the atmospheric loss cone are clearly evident at the same locations as the ion peaks. The narrow ion pitch-angle distributions evident in Figure 1 (e.g., FWHM $\approx 10°$ for the proton peaks) are indicative of an acceleration mechanism which primarily energizes the parallel component of the ion velocity vector. A possible mechanism of this type is a dc electric field with a component parallel to the geomagnetic

field and, as we will see below, a detailed analysis of the ion and electron distribution functions in selected events shows that such electric fields do occur on auroral geomagnetic field lines at high altitudes.

An example of an observation of the second class of ion acceleration mechanism is shown in Fig. 2. These data were acquired in the polar cusp at an altiutde of 7600 km. One sees in Figure 2 a latitudinally extended region of upward-flowing oxygen ions with a "conical" pitch-angle distribution, i.e., having a minimum along the direction of the geomagnetic field. Pitch-angle distributions of this type are expected if the ion acceleration mechanism acts primarily on the perpendicular component of the ion velocity, and at an altitude substantially below that at which the ions are observed. The initial 90° peaked pitch-angle distribution then folds into the observed conical distribution under the action of the first adiabatic invariant. According to this model the ions shown in Figure 2 were accelerated in the altitude region of 4000-5000 km. A possible mechanism resulting in such angular distributions is acceleration by means of ion cyclotron waves.

15 SEPTEMBER 1976 EVENTS

Many of the auroral acceleration events detected by the S3-3 satellite, especially those occurring during active times, are characterized by rapid temporal variations (determinable by differences in the electric potential at altitudes below the satellite as measured by the rapidly moving electrons and the slowly moving ions) and by overlapping and complex spatial structures. In an initial attempt to determine some of the essential features of the structures, two events have been selected for detailed analysis which show evidence for a relative lack of such complicating features and which have a latitudinal scale size suitable for repeated pitch-angle scans by the relatively slowly spinning S3-3 spacecraft. One of these events at 1058 UT on 15 September 1976 has been described in detail by Cladis et al. (1977) and Cladis and Sharp (1977a,b) and, in view of the constraints on the length of this presentation, will not be further discussed here. Survey plots showing the overall characteristics of the second of these events are presented in Figure 3.

The top three panels show, on a logarithmic scale, the summed count rates from the 3 ion spectrometers from ions with the mass-per-charge ratios indicated. The instrument pitch angle is shown in the center panel and the lower four panels show the electron data (see Table 1 for energy ranges). Along the abscissa are given Universal Time (SYST) geographic longitude and latitude, altitude (km), invariant latitude and magnetic local time. An examination of Figure 2 shows an "event" with a relatively symmetric pattern of fluxes. Downward streaming ($\sim$ 100 eV) electrons with a sharply peaked pitch angle distribution form the borders. The central region is characterized by an enhanced flux level of $\sim$ 1 keV electrons with dramatically enlarged loss cones and upstreaming ions (primarily protons in this example) evidencing a parallel electric potential drop below the satellite of about 1 kilovolt in magnitude. The presence of a parallel dc electric field above the satellite in the central portion of the structure is indicated by the reduced level of the CMEA fluxes and the symmetry between the upward and downward moving soft ($E \sim 100$ eV) electrons. In this interpretation the primary electrons have been accelerated out of the energy range of the DMEA detector by a potential difference above the spacecraft of magnitude $\phi_A > 0.24$ kV. The upward moving secondary electrons in the energy range of CMEA produced in the atmosphere by the incident primary beam, are reflected by the parallel electric field above the spacecraft giving rise to the observed symmetry. Another important indicator of a dc electric field above the spacecraft is the presence of minima at 90° in the pitch-angle distributions of the primary (CMEB) electrons. The equation for the first adiabatic invariant for these particles is:

$$\frac{B_1}{E_1 \sin^2 \alpha_1} = \frac{B_2}{(E_1 - e\phi_A) \sin^2 \alpha_2}$$

where B is the intensity of the geomagnetic field. E is the electron energy and α is their local pitch angle. The subscript 1 refers to the altitude at the upper edge of the parallel electric field structure and the subscript 2 refers to the satellite altitude. By setting $\alpha_1 = 90°$ in this equation we have a relationship between the angular width of the observed 90° minimum in the pitch-angle distribution and the vertical extent of the parallel electric field structure above the spacecraft (through B_1). The details of the calculations leading to the determination of this parameter are beyond the scope of this brief report. The results for both the event illustrated and the event analyzed by Cladis and Sharp (1977a,b) are that this vertical dimension is inferred to be greater than 1000 km.

RELEVANCE TO SPACECRAFT CHARGING

The presence of sharply peaked ion and electron pitch-angle distributions such as have been described here have implications with respect to the electrostatic charging of spacecraft systems (Johnson et al., 1977). An observed source of spacecraft malfunctions is the differential electrostatic charging of adjacent insulated surfaces leading to high-voltage discharges and accompanying material damage and electromagnetic interference (Rosen, 1975).

If an anisotropic field-aligned ion flux is incident on a spacecraft with a hole in the outer skin, then a non-conducting surface on a component inside the skin and on the same magnetic field line as the hole will become positively charged providing the hole subtends an angle

from the component surface equal to or less than the pitch-angle range over which the positive ion flux is larger than the electron flux. Assuming that the electron flux is higher than the ion flux at the larger pitch angles (which is typical) then a large negative potential could be formed on the component surface adjacent to a large positive potential. This configuration is illustrated schematically in Figure 4, and to simplify this example, the secondary electron emission from the surface is assumed to be negligible. The surface position L on the component lies along the magnetic field line through the hole in the spacecraft skin. Angles l_1 and l_2 are taken to be less than the pitch-angle range over which the ion flux is greater than the electron flux so that a positive potential will occur at position L. Position N illustrates a surface region at angles between n_1 and n_2 to the magnetic field direction where the electron flux is larger than the ion flux. At this position a negative potential will occur. At some position, M, between N and L the electron and ion fluxes will be equal and a zero potential will occur. It can be seen that the surface charging at each position on the surface is related to the pitch angles subtended at the hole in the skin and thus, in analogy to pinhole cameras for electromagnetic radiations, this will be referred to as the "pinhole camera charging effect". Although it has been illustrated for a net positive flux along the field line, an anisotropic electron flux will also produce a potential gradient across the surface in essentially the same way.

CONCLUSIONS

The ONR low-energy particle experiment on the S3-3 satellite is providing detailed observations of the ion and electron energy and pitch-angle distributions within the ionospheric structures responsible for at least some types of auroral acceleration processes.

For two such structures which have been analyzed in detail, a geometry is inferred which has many properties consistent with the oblique electrostatic shocks predicted by Swift (1975) to be the cause of auroral arcs and "inverted V" events. The observed structures have a latitudinal extent of $\sim$ 300 km, a vertical extent greater than 1000 km, and contain field-aligned electrostatic potentials of the order of several kilovolts. The highly field-aligned pitch-angle distributions of ions and electrons resulting from accelerations within these structures have particular significance with respect to differential charging phenomena on high-altitude spacecraft through the "pinhole camera effect".

ACKNOWLEDGMENTS

This research has been principally supported by the Office of Naval Research under Contract N00014-72-C-0234. Additional support has been provided by the Lockheed Independent Research Program.

REFERENCES

Cladis, J. B., and R. D. Sharp, "Electrostatic Potential Differences Along Magnetic Field Lines Inferred from Satellite Measurements of Electron and Ion Distributions," EOS, 58, 473, 1977a.

Cladis, J. B., and R. D. Sharp, "Distribution of Electrostatic Potential Along Magnetic Field Inferred from Observations of Ion and Electron Fluxes," EOS, 58, 716, 1977b.

Cladis, J. B., L. L. Newkirk, M. Walt, G. T. Davidson, and W. E. Francis, "Investigation of Ionospheric Disturbances," Report No. DNA-4225F, Defense Nuclear Agency, Washington, D. C. 20305, 28 January 1977.

Evans, D. S., "Evidence for Low-Altitude Acceleration of Auroral Particles," in Physics of the Hot Plasma in the Magnetosphere, edited by B. Hultqvist and L. Stenflo, pp. 319-340, Plenum Publishing Company, New York, New York, 1976.

Gurnett, D. A., "Electric Field and Plasma Observations in the Magnetosphere," in Critical Problems of Magnetospheric Physics, edited by E. R. Dyer, IUCSTP Secretariat, National Academy of Sciences, November 1972.

Haerendel, G., "Observations of Electrostatic Acceleration in the Magnetosphere," paper presented at the International Symposium on Solar Terrestrial Relationships, sponsored by the American Geophysical Union, Boulder, Colorado, June 1976.

Johnson, R. G., R. D. Sharp, and E. G. Shelley, "Composition of the Hot Plasma near Geosynchronous Altitude," Proceedings of the Spacecraft Charging Technology Conference, U. S. Air Force Academy, Colorado Springs, Colorado, 27-29 Oct. 1976, in press.

Mizera, P. F., and J. F. Fennel, "Signatures of Electric Fields from High and Low Altitude Particle Distributions," Geophys. Res. Letters, 4, 311, 1977.

Mozer, F. S., C. W. Carlson, M. K. Hudson, R. B. Torbert, B. Parady, J. Yatteau, and M. C. Kelley, "Observations of Paired Electrostatic Shocks in the Polar Magnetosphere," Phys. Rev. Letters, 38, 292, 1977.

Reed, R. D., E. G. Shelley, J. C. Bakke, T. C. Sanders, and J. D. McDaniel, "A Low-Energy Channel Multiplier Spectrometer for ATS-E," IEEE Trans. Nucl. Sci., NS-16, 359, 1969.

Rosen, A., "Large Discharges and Arcs on Spacecraft," Astronautics and Aeronautics, 13, 36, 1975.

Sharp, R. D., R. G. Johnson, and E. G. Shelley, "Observations of an Ionospheric Acceleration Mechanism Producing Energetic (keV) Ions Primarily Normal to the Geomagnetic Field Direction,"

J. Geophys. Res., 82, 3324, 1977.

Shelley, E. G., R. G. Johnson, and R. D. Sharp, "Satellite Observations of Energetic Heavy Ions during a Geomagnetic Storm," J. Geophys Res., 77, 6104, 1972.

Shelley, E. G., R. D. Sharp, and R. G. Johnson, Satellite Observations of an Ionospheric Acceleration Mechanism," Geophys. Res. Letters, 3, 654, 1976.

Swift, D. W., "On the Formation of Auroral Arcs and the Acceleration of Auroral Electrons," J. Geophys. Res., 80, 2096, 1975.

Table 1

DETECTOR CHARACTERISTICS

Detector	Particle	Energy (E, in keV) or Energy-Per-Unit-Charge	$\frac{G\Delta E}{(cm^2\text{-sec-str})}$
CMEA	Electrons	0.07 → 0.24	1.2×10^{-6}
CMEB	Electrons	0.35 → 1.1	6.5×10^{-6}
CMEC	Electrons	1.6 → 5.0	1.9×10^{-5}
CMED	Electrons	7.3 → 24	6.5×10^{-5}
CXA1	Ions	0.50, 0.68, 0.94, 1.28	Depends on ion species $\approx 7 \times 10^{-5}$ E
CXA2	Ions	1.76, 2.4, 3.3, 4.5	
CXA3	Ions	6.2, 8.5, 11.6, 16.0	

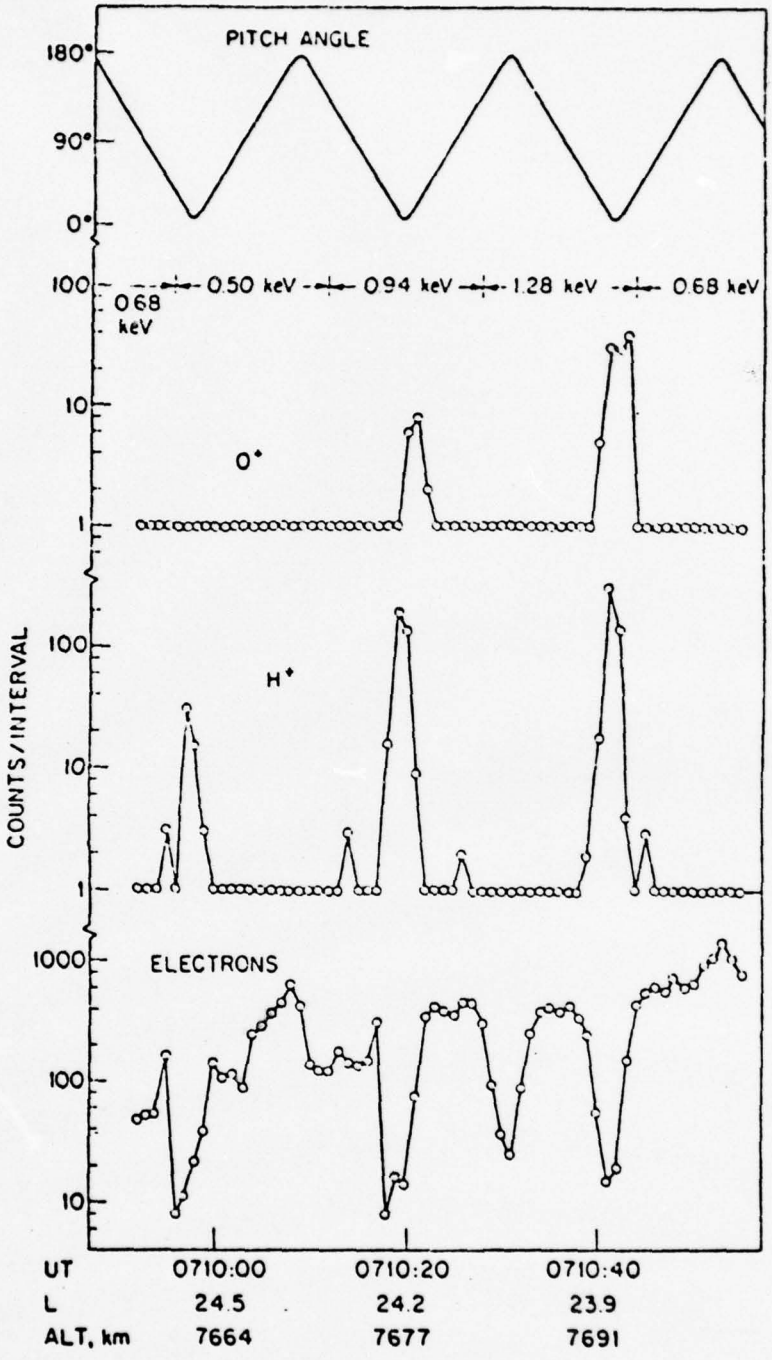

Figure 1. Data from Revolution 67 on 17 July 1976. The upper panel shows the pitch angle of the instrument axis. The two center panels show data from the mass spectrometer at the indicated energies, and the lower panel shows electron fluxes in the energy range from 0.37 to 1.28 keV.

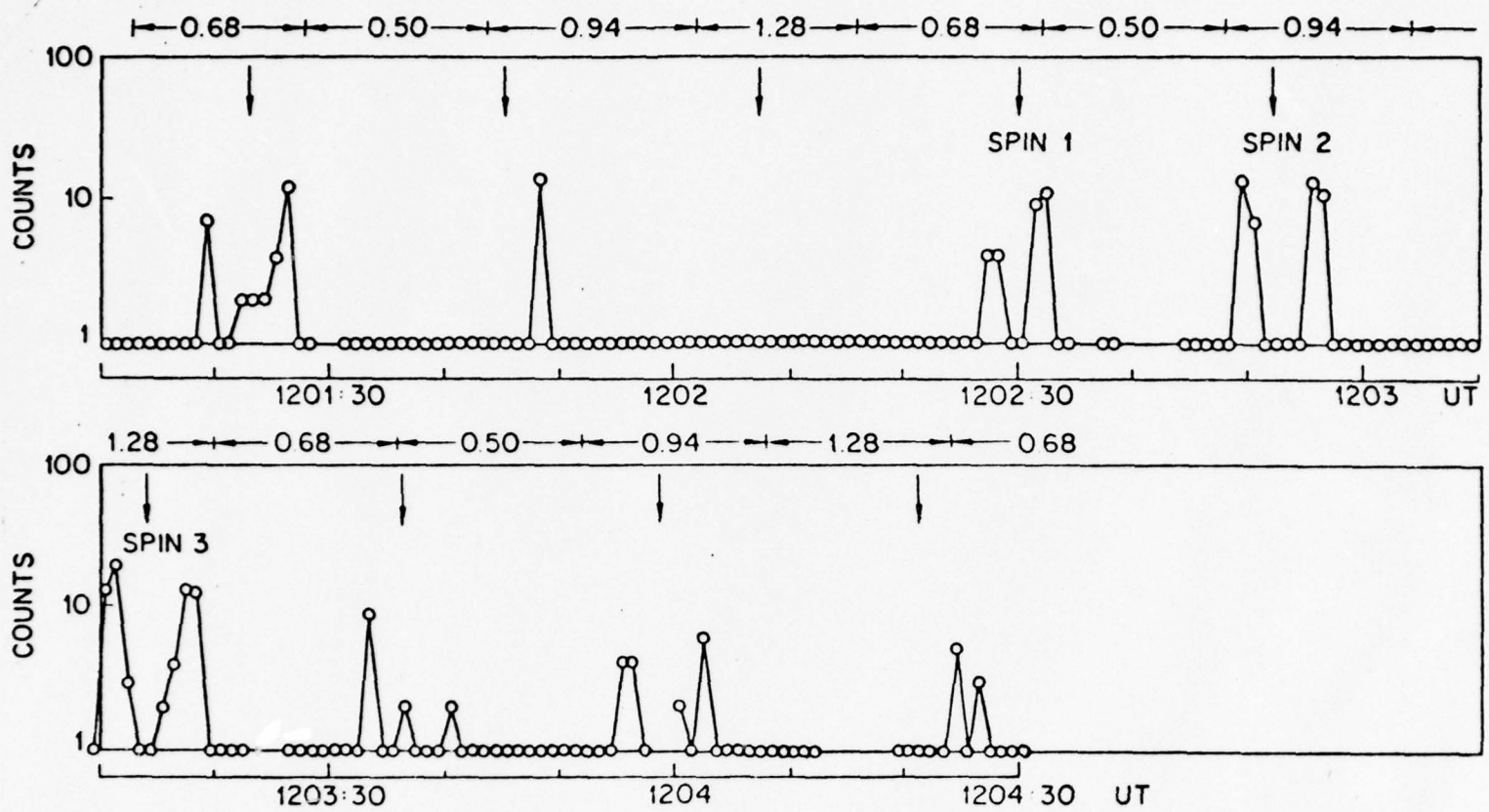

Figure 2. O^+ data from the lowest energy mass spectrometer (CXA1) at the times indicated, on 29 July 1976. The arrows indicate those times (once per spin) when the instrument was oriented nearly parallel to the magneitc field and pointing downward. The numbers above the panels are the energy-per-unit-charge setting of the spectrometer (in keV).

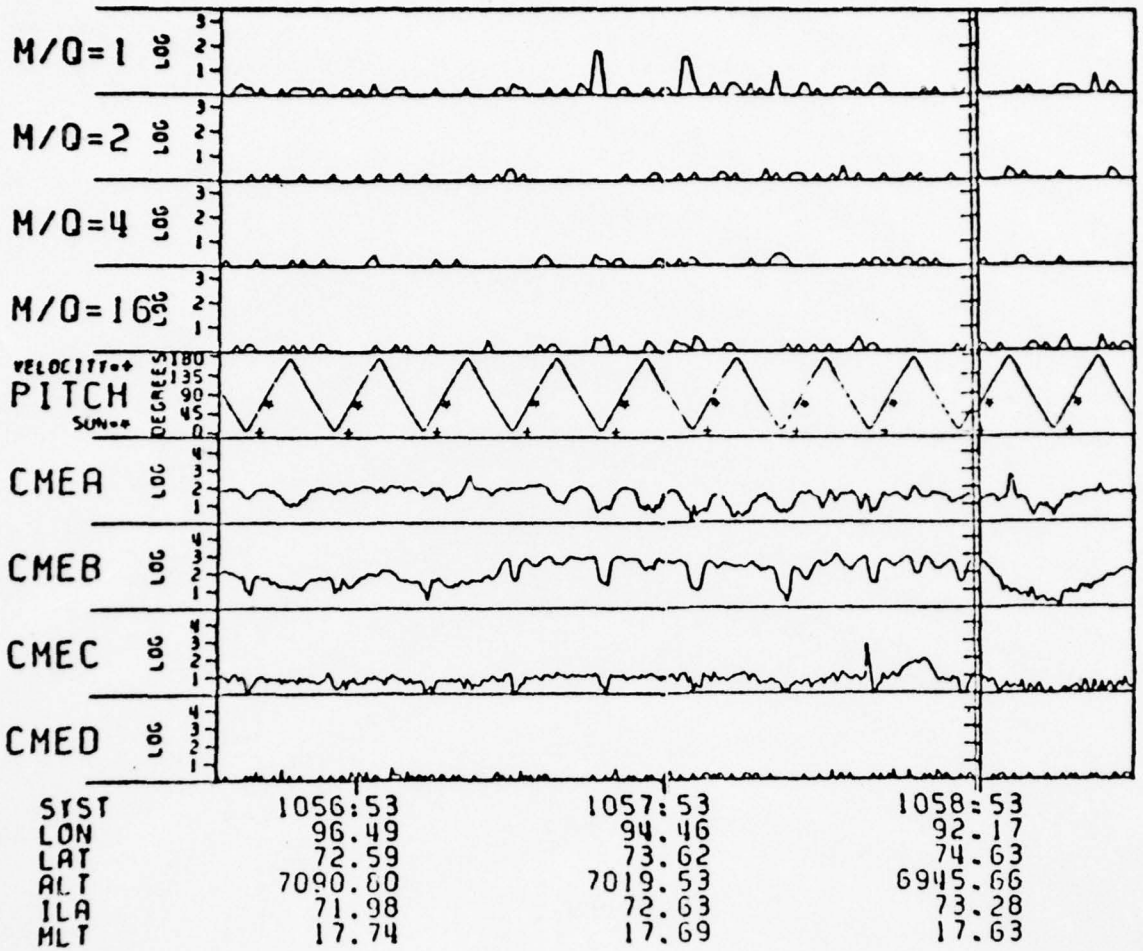

Figure 3. Survey plots of ion and electron data during an auroral acceleration event on 15 September 1976. See text for details.

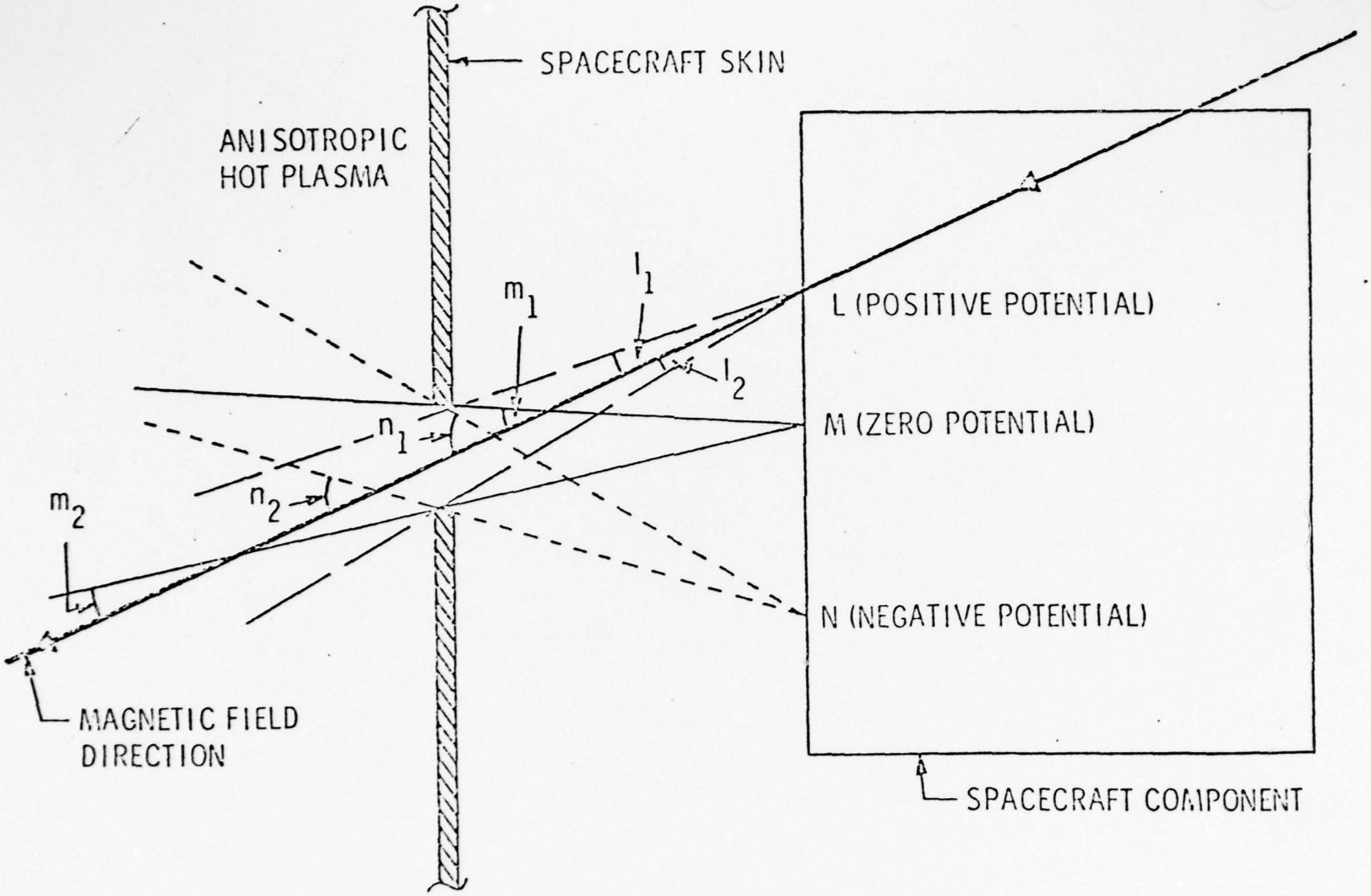

Figure 4. A schematic drawing illustrating the geometry for the pinhole camera charging effect in anisotropic hot plasmas.

OBSERVATIONS OF IONS OF IONOSPHERIC ORIGIN IN THE STORM-TIME RING CURRENT

R. G. Johnson, R. D. Sharp, and E. G. Shelley

Lockheed Palo Alto Research Laboratory, Palo Alto, California 94304

Abstract. O^+, He^+, and H^+ ions in the energy range 0.5 to 16 keV have been observed in the storm-time ring current with an energetic ion mass spectrometer aboard the polar-orbiting S3-3 satellite. During the main phases of the 29 December 1976, 6 April 1977, and 19 April 1977 magnetic storms, the O^+ number density within the instrument energy range in the inner ring current (L = 2.8-4.0) was larger than the H^+ density in the altitude range from about 5000-7000 km. At two days after the main phase of the 29 December 1976 storm, O^+ was still the dominant ion at MLT = 14.5 hours in the L = 2.6-3.4 range at altitudes near 6000 km.

Introduction

This letter is a preliminary report on the first direct observation of ions of ionospheric origin in the storm-time ring current. The data were obtained with a satellite-borne energetic ion mass spectrometer in the energy range 0.5 to 16 keV and at altitudes up to 8000 km. Data are presented from the three largest magnetic storms which have occurred since the satellite S3-3 started acquiring data in July 1976. In view of the constraint of the length of this letter, the main phases of the storms are emphasized here, but one example of the composition during the recovery phase is also presented.

The discovery of O^+ ions precipitating from the magnetosphere with energies up to 12 keV was reported by Shelley et al. (1972) and the ions were inferred to be of ionospheric origin. However, no measurements on the trapped component of the fluxes were obtained because of the spacecraft orientation. Several aspects of the morphology of these O^+ ions have been investigated and their possible relationships to the storm-time ring current have been discussed previously (Shelley et al., 1972; Johnson et al., 1976a; Sharp et al., 1976, 1977).

Based on considerations of ion lifetimes against charge exchange in the ring current regions, Tinsley (1976) and Lyons and Evans (1976) conclude that existing data were inconsistent with protons being the dominant ring-current ion species but that the data were consistent with He^+ being the dominant species during the recovery phases of storms. These conclusions are in contrast to earlier analytical work by Smith et al. (1976) and by Berko (1975) who concluded that their data were consistent with protons as the dominant ions during the recovery phases of the storms investigated. More complete reviews of the energetic ion composition in the magnetosphere have recently been made by Fritz (1976) and Johnson et al. (1976a).

Copyright 1977 by the American Geophysical Union.

Paper number 7L0781.

Observations

The ion composition measurements were made with an energetic ion mass spectrometer aboard the polar-orbiting S3-3 spacecraft which has perigee near 350 km and apogee near 8000 km. The spacecraft is spinning at 3 rpm with the spin axis normal to the orbital plane and with the instrument view directions in the orbital plane. The instrument contains 3 ion mass spectrometers and 4 electron spectrometers similar to those previously described (Shelley et al., 1972; Reed et al., 1969). Each ion spectrometer acquires a 30-channel mass-per-unit-charge spectrum every second. Every 16 seconds the energy-per-unit-charge setting for each spectrometer is stepped to one of the four values, allowing a 12-point energy spectrum to be acquired every 64 seconds. Each spectrometer on Step 1 is in the lowest energy step, etc. The energy-per-unit-charge values are 0.5, 0.68, 0.94, and 1.28 keV for spectrometer #1; 1.76, 2.4, 3.3, and 4.5 keV for spectrometer #2; and 6.2, 8.5, 11.6, and 16.0 keV for spectrometer #3. The four broadband electron channels span the energy ranges 0.07 to 0.24 keV, 0.35 to 1.1 keV, 1.6 to 5.0 keV, and 7.3 to 24 keV.

Figure 1 shows Dst for the magnetic storms on 29 December 1976, 6 April 1977, and 19 April 1977. The locations of main phase data to be discussed are identified by the arrows for spacecraft revolutions 1397, 2196, and 2297. The approximate magnetic local times for the centers of the main phase data intervals to be presented are 2.2, 21.0, and 21.4 hours, respectively. As an example of the data, a survey plot for the first data acquisition through the ring-current region during the 29 December 1976 magnetic storm is shown in Figure 2 for satellite revolution 1397. The abscissa shows universal time on 29 December 1976, altitude in kilometers, invariant latitude, magnetic local time, and L-shell. The four lowest panels show the logarithm of the counts per half-second counting interval for the electron spectrometers with the lowest energy being CMEA, etc. The panel labeled PITCH shows the pitch angle of the look direction of the spectrometers. The next four panels show the logarithm of the counts from ions with M/Q = 1, 2, 4, and 16 summed once per second from selected output channels from all three of the ion mass spectrometers, giving an approximate measure of the relative flux of the relevant species. The top panel shows the energy step of each of the three ion mass spectrometers. The time spent on each energy step (16 seconds) is slightly shorter than the satellite spin period (20 seconds). In the region L = 3 to 4, trapped fluxes of H^+ and O^+ ions are easily identified by comparing the M/Q = 1 and 16 responses with the pitch-angle plot. Above about L = 4, significant proton precipitation and weak O^+ precipitation are occurring as seen from the filling of the loss cone.

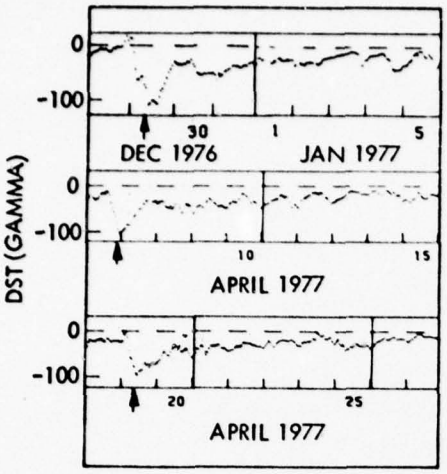

Fig. 1. Provisional Dst values for the 29 Dec. 1976, 6 April 1977, and 19 April 1977 magnetic storms. Arrows indicate the universal times of the satellite passes.

An analysis of the mass spectrums shows that the response seen in the M/Q = 2 panel is all background counts within the statistical uncertainties, but the response seen in the M/Q = 4 panel results from both background counts and low-level He^+ counts. Electron precipitation is seen in all the electron channels throughout the region except for the highest energy channel in the region below about L = 4. The O^+ and H^+ fluxes observed for revolutions 2196 and 2297 are comparable to those illustrated in Figure 2 and extend to somewhat lower L-shells.

Examples of the mass-per-unit-charge spectrums of the ions in the inner ring-current region are shown in Figure 3 for each of the three mass spectrometers for satellite revolutions 1397, 2196, and 2297. The L-shell intervals were selected to start near the low-latitude edge of the principal fluxes and to extend outward to L = 4, or for revolution 2196, until the backgrounds in the spectrometers due to the outer-belt electrons became comparable to the O^+ peaks in the mass spectrums. Data from all measured pitch angles are included. In two of the panels, the spectrometer outputs are summed over the four energy steps to improve the counting statistics. The relatively large quantities of the O^+ ions are evident in each case and smaller amounts of He^+ are seen in revolutions 2196 and 2297. The equatorial pitch-angle ranges corresponding to the 90° pitch angles for the above L-shell ranges are 15 to 21 degrees, 20 to 41 degrees, and 15 to 31 degrees for revolutions 1397, 2196, and 2297, respectively. On revolution 2196, much lower intensity O^+ and H^+ fluxes were also observed down to L = 2.6 at 90° pitch angle, corresponding to 50 degrees equatorial pitch angle

Figure 4 shows the energy distributions for the O^+ and H^+ ions in the same L-shell ranges as for Figure 3. The pre-storm fluxes in these L-shell ranges were undetected above the local backgrounds which can be generally assessed from the regions between the peaks in Figure 3. For revolutions 1397 and 2297 it is seen in Figure 4 that the H^+ fluxes are somewhat higher than the O^+ fluxes and for revolution 2196 the fluxes are seen to be comparable. The H^+ spectrum is noticeably harder than the O^+ spectrum for revolution 1397, but the spectrums are similar for the other two revolutions. The number densities integrated over the energy range of the experiment corresponding to these fluxes are given in Table 1. It is seen that in each case the O^+ number density exceeds the H^+ number density. The O^+ number densities also exceeded the He^+ number densities by more than a factor of ten in each case.

Two days after the beginning of the 29 December 1976 storm, data were acquired at about 0850 UT hours on 31 December in the inner ring-current region near 6000 km at a magnetic local time of 14.5 hours. The O^+ and H^+ fluxes were more than a factor of ten lower than the peak fluxes observed during the main phase of the storm, and were observed only in the two lower energy spectrometers. Adequate signal-to-background counts were obtained in the L-shell range 2.6 to 3.4 to produce the mass spectrum shown in Figure 5. O^+

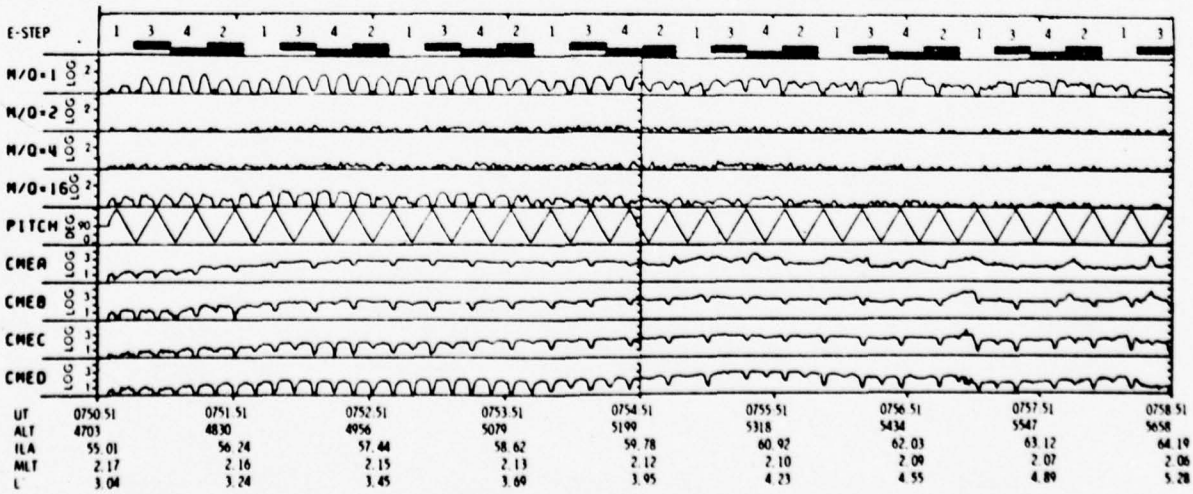

Fig. 2. A survey plot of the ion and electron counting rates on 29 December 1976 during satellite revolution 1397. The parameters are discussed in the text.

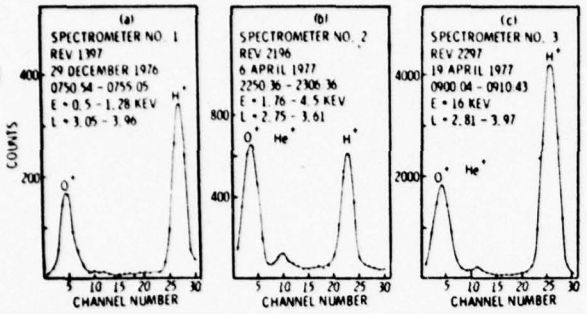

Fig. 3. Examples of mass spectrums from the three ion spectrometers during the main phases of the 29 December 1976, 6 April 1977, and 19 April 1977 magnetic storms.

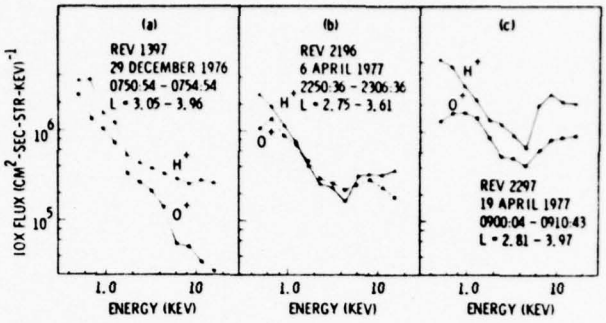

Fig. 4. Energy distributions for O^+ and H^+ during the main phases of the 29 December 1976, 6 April 1977, and 19 April 1977 magnetic storms.

is still found to be the dominant ion. The spectrum is summed over the 4 energy steps to improve the counting statistics. The equatorial pitch-angle range for the 90° pitch angles measured in this L-shell range is from 21° to 32°.

Discussions and Conclusions

The data from the early portions of the main phases of the storms were selected for presentation with the view that this was the most favorable time period to observe the composition of the ions being injected into the inner ring current regions. At least at these times the effects on the composition due to charge exchange loss processes (Tinsley, 1976) would be minimized, even though the effects of transport processes remain to be investigated. At the present stage of the analysis, the most significant aspect of the observations is the large number density ratios of O^+ to H^+ ions and O^+ to He^+ ions in the inner ring current regions during the main phases of the storms. In view of the low density and high charge state of oxygen ions in the solar wind (Bame et al., 1970) and the direct satellite observations of large fluxes of upward streaming energetic ionospheric ions, including O^+ ions (Shelley et al., 1976; Johnson et al., 1976b; and Sharp et al., 1977), it is concluded from the high O^+ to H^+ density ratios in the present data that the ionosphere is a major contributor to the main phase ring current in the energy and pitch-angle ranges of the observations. It is recognized that the present observations cover only limited ranges in energy distributions and in equatorial pitch angles. However, the equatorial pitch angle range of the main phase observations extended to 50°, and a preliminary analysis of the pitch-angle distributions shows no evidence for strong gradients in the distributions near the upper ends of the equatorial pitch-angle ranges. In particular, there was no evidence for the "source cone" distributions of the type observed by Mauk and McIlwain (1975) on the ATS-6 satellite at geosynchronous altitude ($L \approx 6.6$). From the present data set it is not feasible to determine the latitude, local time, etc., of the ionospheric source region nor to identify the acceleration and transport processes involved. These areas will be investigated when the more extensive satellite data sets from these storms are available.

Although the energy spectrums for the local evening data shown in Figures 4(b) and 4(c) for the two April storms are somewhat similar and show evidence of two components, it should be emphasized that the energy spectrums varied significantly within the L-shell intervals, and the details of the averaged spectrums may have little significance. However, with respect to the ion composition, it should be noted that in these two cases the relatively large O^+ fluxes at 16 keV result in the O^+ number densities exceeding the H^+ number densities at 16 keV, thus also indicating a significant ionospheric contribution to ion fluxes at the upper end of the energy spectrums. This is in contrast to the morning sector data shown in Figure 4(a) for the December storm which shows a rapidly-falling O^+ spectrum and the O^+ number density is only about one-half of the H^+ number density at 16 keV. The significance of the

TABLE 1. Number Densities

Revolution	L-Shell Range	O^+ Number Density, N_{16} (cm^{-3}) (0.5 - 16 keV)	H^+ Number Density, N_1 (cm^{-3}) (0.5 - 16 keV)	N_{16}/N_1
1396	3.05 - 3.96	2.9	1.4	2.1
2196	2.75 - 3.61	3.3	1.1	3.0
2297	2.81 - 3.97	7.1	4.6	1.5

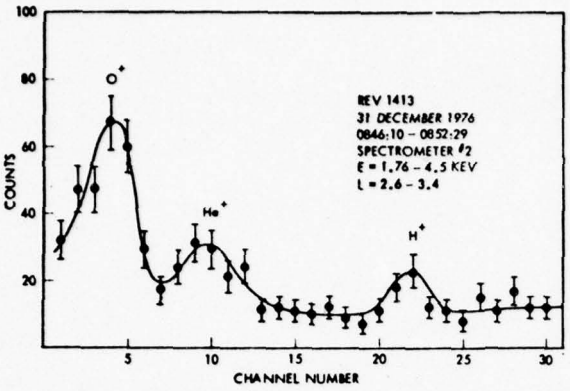

Fig. 5. An example of the mass spectrum during the recovery phase of the 29 December 1976 magnetic storm.

local time or storm to storm differences in the spectrums remains to be investigated.

The most obvious characteristic of the recovery phase mass spectrum shown in Figure 5 is that the dominant species is O^+. In comparison to the main phase mass spectrums shown in Figure 3 there is an enhancement of He^+ and depletion of H^+ relative to the O^+. This is a preliminary result based on the limited data shown but is qualitatively consistent with expectations based on charge exchange (Tinsley 1976).

In view of the large fluxes of ionospheric ions observed during the main phases of the three storms discussed above, we conclude that the injection, acceleration, transport, and loss processes for the storm-time ring current should now be re-evaluated with consideration of an ionospheric source term.

Acknowledgments. This work was supported by the Office of Naval Research (ONR) under Contract N00014-72-C-0234. We would like to thank T. C. Sanders, E. Hertzberg, J. D. Matthews, and J. D. McDaniel for their contributions to the design and construction of the spectrometer and D. L. Carr for his assistance with the data reduction. We also thank Commander R. Oberle, ONR Project Officer, for his staunch support of this experiment and for his extraordinary efforts which were required to include the ion mass spectrometer in the S3-3 payload late in the program.

References

Bame, S. J., J. R. Asbridge, A. J. Hundhausen, and M. D. Montgomery, Solar wind ions: $^{56}Fe^{+12}$, $^{28}Si^{+7}$, $^{28}Si^{+8}$, $^{28}Si^{+9}$, and $^{16}O^{+6}$, J. Geophys. Res., 75, 6360, 1970

Berko, F. W., L. J. Cahill, Jr., and T. A. Fritz, Protons as prime contributors to the storm-time ring current, J. Geophys. Res., 80, 3549, 1975.

Fritz, T. A., Ion composition, in Physics of Solar Planetary Environments, Vol. II, D. J. Williams, Editor, American Geophysical Union, Washington, D. C., p. 716, 1976.

Johnson, R. G., R. D. Sharp, and E. G. Shelley, Composition of the hot plasmas in the mangetosphere, in Physics of the Hot Plasma in the Magnetosphere, B. Hultqvist and L. Stenflo, Editors, Plenum Publ. Corp., N.Y., N.Y., p. 45, 1976a.

Johnson, R. G., R. D. Sharp, and E. G. Shelley, Characteristics of upward-flowing energetic (keV) ionospheric ions during a magnetically disturbed period, EOS, 57, 993, 1976b.

Lyons, L. R., and D. S. Evans, The inconsistency between proton charge exchange and the observed ring current decay, J. Geophys. Res., 81, 6197, 1976a.

Mauk, B. H., and C. E. McIlwain, ATS-6 UCSD auroral particles experiment, IEEE Trans. on Aerospace and Electronic Systems, Vol. AES-11, 1125, 1975.

Reed, R. D., E. G. Shelley, J. C. Bakke, T. C. Sanders, and J. D. McDaniel, A low-energy channel-multiplier spectrometer for ATS-E, IEEE Trans. Nucl. Sci., NS-16, 259, 1969.

Sharp, R. D., R. G. Johnson, and E. G. Shelley, The morphology of energetic O^+ ions during two magnetic storms: Temporal variations, J. Geophys. Res., 81, 3283, 1976.

Sharp, R. D., R. G. Johnson, and E. G. Shelley, Observation of an ionospheric acceleration mechanism producing energetic (keV) ions primarily normal to the magnetic field direction, J. Geophys. Res., 82, 3324, 1977.

Sharp, R. D., E. G. Shelley, and R. G. Johnson, A search for helium ions in the recovery phase of a magnetic storm, J. Geophys. Res., 82, 2361, 1977.

Shelley, E. G., R. G. Johnson, and R. D. Sharp, Satellite observations of energetic heavy ions during a geomagnetic storm, J. Geophys. Res., 77, 6104, 1972.

Shelley, E. G., R. D. Sharp, and R. G. Johnson, Satellite observations of an ionospheric acceleration mechanism, Geophys. Res. Letters, 3, 654, 1976.

Smith, P. H., R. A. Hoffman, and T. A. Fritz, Ring current proton decay by charge exchange, J. Geophys. Res., 81, 2701, 1976.

Tinsley, B. A., Evidence that the recovery phase ring current consists of helium ions, J. Geophys. Res., 81, 6193, 1976.

(Received August 8, 1977;
accepted August 19, 1977.)

THE LATITUDINAL, DIURNAL, AND ALTITUDINAL DISTRIBUTIONS OF UPWARD FLOWING ENERGETIC IONS OF IONOSPHERIC ORIGIN

A. G. Ghielmetti*, R. G. Johnson, R. D. Sharp, and E. G. Shelley

Lockheed Palo Alto Research Laboratory, Palo Alto, California 94304

November 1977

Accepted for publication in
Geophysical Research Letters

*Visiting scientist from University of Bern, Physikalisches Institut, Bern, Switzerland

Abstract. Upward flowing fluxes of energetic (0.5-16 keV) H^+ and O^+ ions are frequently observed by the ion mass spectrometer on the polar-orbiting S3-3 satellite. Data obtained on the first ∿370 orbits have been used to derive the occurrence frequency of these fluxes. The upward acceleration of ionospheric ions to keV energies is a persistent phenomenon generally occurring in a zone closely associated with the statistical auroral oval. Upward flowing ion events with flux above ∿2 x 10^6 keV/(cm^2 sec ster keV) are observed in more than 60% of the orbits. A strong dawn-dusk asymmetry is found in the frequency of occurrence with the maximum in the dusk sector. The probability of observation increases with altitude up to apogee (8000 km) indicating that the main energization takes place preferentially at altitudes above ∿1 R_E.

Introduction

Evans (1975) has recently summarized the observational evidence for acceleration of auroral electrons at low altitudes. He noted that the absence of a comparable body of field-aligned ion observations could be due to a preferential upward direction for the parallel electric field. More recently intense fluxes of narrowly collimated upward flowing ions have been discovered over the polar ionosphere (Shelley et al., 1976). These fluxes have been interpreted as evidence for a parallel electric field acceleration (Sharp et al., 1977; Mizera and Fennell, 1977). Upward flowing conical distributions having a minimum in the magnetic field direction have been reported in the same general regions (Sharp et al., 1977) and interpreted as resulting from perpendicular acceleration. In this letter we present the results of a preliminary statistical study of the frequency of occurrence of upward flowing ion (UFI) events of both types in the polar ionospheres. The purpose of this work is to determine the spatial location of the ion-acceleration regions, their absolute frequency of occurrence and to examine briefly their relation to auroral phenomena.

Experiment Description

The data used in this study were acquired by a set of 3 energetic ion-mass spectrometers on the polar-orbiting S3-3 (1976-065B) satellite. The

three spectrometers operate simultaneously at different energy/charge levels, producing a 12-point energy spectrum in the range from 0.5-16 keV in 64 seconds. A complete mass scan from mass/charge 1 through 32 is acquired once every second. The instrument was described in more detail in a previous publication (Sharp et al., 1977). The sensors are mounted with view direction perpendicular to the orbital plane and spinning at a rate of approximately 3 RPM. The S3-3 satellite is in an elliptical polar orbit (8000 km by 250 km, 97.5° inclination) with a period of ∿3 hours. The orbit precesses at a rate of about one hour in local time per 20 days and the line of apsides drifts at a rate of about 1°/day in the orbital plane. Data from ∿370 satellite orbits have been included in this analysis covering the time period from July 1976 to February 1977. This period was relatively quiet magnetically with the three hourly Kp value being ≤ 3 in 76%, $3 < Kp \leq 5$ in 21% and $Kp > 5$ in 3% of the orbits.

For statistical purposes we have subdivided the polar regions between 60 and 84 degrees invariant latitude (ILA) into unit bins of size 2° ILA by 3 hours magnetic local time (MLT) by 1000 km altitude. A bin is defined to have been sampled if at least one complete pitch angle scan is acquired while the satellite passes through it. We define a UFI event as the occurrence of at least one observation within a unit bin of an anisotropic pitch-angle distribution having a maximum in the upward moving direction. In addition, we require that the energy flux exceed the sensitivity threshold of $\sim 2 \times 10^6$ keV/(cm^{2}sec ster keV) and the penetrating energetic electron background. Since the pitch angle scans do not always extend to 0°, conical distributions peaking at less than 10° to the field line often cannot be distinguished from field aligned ones. In addition, both kinds of distributions are consistent with a combined parallel and perpendicular acceleration process. Thus for this analysis no distinction is made between field aligned and conical events. A total of about 8500 samples were obtained in the period of this analysis and about 380 UFI events were observed. The probability of occurrence is defined as the ratio of the number of UFI events to the number of samples within a bin.

Results

Protons and singly charged oxygen ions are the principal ion species observed in UFI events. They occur with about equal probability and have energies varying over the full range of the instrument (500 eV to 16 keV). Typical H^+ fluxes are of the order of 5×10^7 ions/(cm^2 sec ster keV) with the maximum flux about an order of magnitude greater. The O^+ fluxes are generally less intense. Helium ion fluxes are rarely observed, and contribute generally less than about 10^{-2} to the total flux. The majority of UFI's have field-aligned pitch angle distributions with typical full widths at 10% of intensity maximum ranging from $\sim$10° to $\gtrsim$120°. Their energy distributions are generally broad, i.e., relative to the energy step separation. Conical pitch-angle distributions are observed relatively more frequently in the O^+ ions and mainly near noon. It should be noted that these angular and energy widths of the field-aligned ion distributions are inconsistent with purely parallel acceleration of cold ionospheric ions suggesting the presence of some perpendicular acceleration process.

The latitudinal extent of the contiguous regions in which UFI events are observed varies from a fraction of a degree to $\sim$8° ILA. In a few cases when the satellite passed obliquely through the dusk side auroral zone, regions of continuous ion upflow were observed with longitudinal extent of several hours in MLT. The overall probability that a region of UFI events is encountered on a satellite pass through the polar auroral zone above an altitude of 4000 km is about 60%.

Latitudinal Distribution. To obtain the average probability of observing a UFI event within a given latitude-MLT sector and above 6000 km, we summed the number of samples and the number of events over the two highest altitude intervals (6000-8000 km). Figure 1 shows the histogram distribution of the probability as a function of invariant latitude and magnetic local time. We see that the UFI events occur within a well-defined latitudinal zone. This zone exhibits a diurnal variation with the centroid moving from $\sim$78° ILA at local noon to $\sim$68° ILA at local midnight. It is wider in the dusk-to-midnight sector ($\sim$15°) than near noon ($\sim$10°). These features are in good correspondence with the statistical auroral oval as derived by Feldstein et al. (1969). Although the observed absolute probability of oc-

currence is somewhat less than that of discrete auroral arcs, it is nevertheless significant ($\gtrsim$30%). This value represents a lower limit on the actual occurrence frequency because of observational limitations due to the slow spin rate and the limited energy and sensitivity range of the instrument. In particular, spatially narrow structures, short-lived events, monoenergetic beams and very narrowly collimated beams ($\lesssim$5°) are likely to be missed. Because of increased telemetry noise in the data from August and September 1976 (35 orbits), some weak UFI events in the 15-21 hr MLT sector may have been obscured. In the two sectors from 0300 to 0900 hr MLT the sampling frequency was inadequate to produce a statistically meaningful latitudinal distribution. Since the coverage in MLT and altitude in the two hemispheres is controlled by the orbit dynamics, biases may result from seasonal effects and variations in magnetic activity. In particular, the 9-12 hour MLT sector was sampled only in the northern hemisphere and mainly during magnetically quiet periods while the 0-3 hr MLT sector was sampled only in the southern hemisphere mainly during magnetically disturbed periods. A preliminary analysis of subdivided data indicates significant differences due to magnetic activity but no evident hemispherical difference.

While occasional UFI events have been observed at latitudes higher than 84° ILA, none were detected below 60° ILA. The detection threshold for ions is often higher at lower latitudes due to penetrating electron background; however, field-aligned ion fluxes typical of the higher latitudes would have been detected. The absence of such events at lower latitudes suggests that the large fluxes of energetic O^+ ions reported in the storm-time ring current as low as 52° ILA (Johnson et al., 1977) are not directly injected onto the field lines from the ionosphere but are transported in from the higher latitude regions.

A comparison of the frequency of occurrence of UFI events in the 21-24 hr sector with the distribution of overhead discrete aurora at solar minimum in the 21-03 hr local time sector (Feldstein et al., 1969) is shown in Figure 2. The UFI event data are renormalized to the maximum probability of the IQSY auroral distribution. Ion data from the 0-3 hr MLT sector are not included because they stem primarily from magnetically active periods. It is seen that the relative distribu-

tion of UFI events and the distribution of discrete auroral forms are essentially the same.

Local Time Distribution. To obtain the relative local time distribution of UFI events we integrated the probability distributions of Figure 1 over invariant latitude. The resultant distribution is displayed in Figure 3. We see that the probability of observing an event is approximately constant from 12 to 24 hours but decreases significantly in the 0 to 12 hour sectors that were covered. Thus, a strong dawn-dusk asymmetry in the occurrence frequency of these ion acceleration events is indicated. Alternatively, the lower probability in the morning hemisphere might be explained by an acceleration process that generally produces UFI events with structures that are more likely to be missed as discussed above.

While auroral frequency distributions obtained from all-sky camera observations do not show clear evidence of a dawn-dusk asymmetry (Feldstein et al., 1969), the DMSP photographs do indicate that discrete auroral forms occur predominately on the evening side (Akasofu, 1975). Strong perpendicular electric fields described as electrostatic shocks are frequently encountered near UFI events (Mozer et al., 1977). The statistical region of occurrence in MLT-ILA space of these shocks (Torbert and Mozer, 1978) is in good agreement with the distribution described here but does not display a clear dawn-dusk asymmetry. Correlations between the location of regions of electrostatic turbulence within which electrostatic shocks are imbedded and discrete auroral arcs have been reported in three cases studied (Torbert and Mozer, 1978). Inverted V electron precipitation events and auroral zone VLF hiss also exhibit a significant dawn-dusk asymmetry being relatively uncommon at dawn (Gurnett and Frank, 1972; Gurnett, 1966; Hughes and Kaiser, 1971). These two phenomena have been found to be correlated with one another (Gurnett and Frank, 1972; and with discrete auroral forms (Ackerson and Frank, 1972; Mosier and Gurnett, 1972). The inverted V events are commonly narrower and have a lower peak electron energy at dawn than at dusk (Frank and Ackerson, 1972). The observed distribution of UFI events suggests that the regions of upward ion-acceleration, downward electron acceleration, and discrete auroral arcs are closely associated, and that these phenomena involve parallel electric fields. The large-scale field-aligned current systems also exhibit a dawn-dusk asymmetry in the

upward directed current density, being generally higher at dusk than at dawn (Potemra, 1977). Although the difference is small, it might be a significant factor in causing the dawn-dusk asymmetry in the UFI events if a current-driven instability is involved in the mechanism responsible for the parallel acceleration of ions.

Altitude Distribution. By summing the probabilities over the latitude range within which 90% of the events occur in each MLT sector, we obtain an average altitude distribution. The average probability $\bar{p}(A)$ that a UFI event occurs at a given altitude (A) and any local time and latitude is defined as

$$\bar{p}(A) = \sum_L \sum_T p(L,T,A)/\text{number of unit bins}$$

where p(L,T,A) is the probability of observation within a given bin at invariant latitude (L), local time (T), and altitude (A). We have not attempted to correct the probability distributions for possible biases resulting from the fact that less time is spent in traversing a bin at lower altitudes. The magnitude of such a correction is dependent on unknown parameters such as the characteristic widths and temporal duration of UFI events; however, the effect is expected to be less than a factor of 2 in the 4000 to 8000 km altitude range. The resultant distribution (Figure 4a) shows that the probability of finding a UFI event increases with altitude up to apogee. Eighty-five percent of the events occur above 5000 km and two-thirds occur above 6000 km. The differential frequency distribution obtained by subtracting probabilities in adjacent altitude regions (Figure 4b) also shows a general increase with altitude, suggesting that the acceleration frequently occurs above 8000 km. These results also imply that the -500 volt equipotential surface is located most frequently at altitudes above 6000 km and only rarely below 4000 km. The altitude region where ions are accelerated appears to coincide well with the inferred source location of auroral kilometric radiation (Gurnett, 1976) and VLF auroral hiss (Gurnett and Frank, 1972).

Summary and Conclusions

A statistical survey of mass spectrometer data from the S3-3 satellite has revealed the existence of an oval-shaped region in the polar ionosphere

where upward acceleration of ionospheric H^+, O^+, and occasionally He^+ ions is occurring. The shape and location of this region are in good correspondence with the statistical auroral oval. These upward flowing ions are a persistent phenomenon with a high frequency of occurrence. The observations are consistent with a common parallel electric field acceleration mechanism producing both discrete auroral arcs and the upward streaming ion fluxes. However, the observed broad energy and pitch-angle distributions suggest that a perpendicular acceleration process is also often involved. The observed dawn-dusk asymmetry implies that upward-directed parallel electric fields involving kV potential drops occur primarily in the dusk hemisphere. In this preliminary study we find no evidence in the ion data for parallel fields with reversed polarity. We can infer from the altitude profile that the main energization of ions to energies above 0.5 keV takes place preferentially at altitudes above 5000 km and probably extends to altitudes above 8000 km. The existence of small parallel potential drops ($\lesssim$0.5 kV) or of weak perpendicular energization at lower altitudes is not inconsistent with these results.

Acknowledgments. The S3-3 satellite experiment was supported by the Office of Naval Research under Contract N00014-72-C-0234. This analysis was partially supported by the Atmospheric Sciences section of the National Science Foundation and the Lockheed Independent Research program. One of us (A.G.) would like to acknowledge the support of the Swiss National Science Foundation.

References

Ackerson, K. L., and L. A. Frank, Correlated satellite measurements of low-energy electron precipitation and ground-based observations of a visible auroral arc, J. Geophys. Res., 77, 1128, 1972.

Akasofu, S.-I., A Study of auroral displays photographed from the DMSP-2 and ISIS-2 satellites, in Physics of the Hot Plasma in the Magnetosphere, B. Hultqvist and L. Stenflo, ed., p. 113, Plenum Press, New York and London, 1975.

Evans, D. S., Evidence for the low-altitude acceleration of auroral particles, in Physics of the Hot Plasma in the Magnetosphere, B. Hultqvist and L. Stenflo, ed., p. 319, Plenum Press, New York and London, 1975.

Feldstein, Y. I., S. I. Isaev, and A. I. Lebedinsky, The phenomenology and morphology of aurorae, in Annals of the IQSY, Vol. 4, pp. 311-348, MIT Press, Cambridge, Mass., 1969.

Frank, L. A., and K. L. Ackerson, Local-time survey of plasma at low altitudes over the auroral zones, J. Geophys. Res., 77, 4116, 1972.

Gurnett, D. A., and L. A. Frank, VLF hiss and related plasma observations in the polar magnetosphere, J. Geophys. Res., 77, 172, 1972.

Gurnett, D. A., A satellite study of VLF hiss, J. Geophys. Res., 71, 5599, 1966.

Gurnett, D. A., The earth as a radio source, in Magnetospheric Particles and Fields, B. M. McCormac, ed., p. 197, D. Reidel, Dordrecht-Holland, 1976.

Hughes, A. R. W., and T. R. Kaiser, VLF Radio emissions and the aurora, in The Radiating Atmosphere, B. M. McCormac, ed., p. 336, D. Reidel, Dordrecht-Holland, 1971.

Johnson, R. G., R. D. Sharp, and E. G. Shelley, Observations of ions of ionospheric origin in the storm-time ring current, Geophys. Res. Lett., 4, 403, 1977.

Mizera, P. F., and J. F. Fennell, Signatures of electric fields from high and low altitude particle distributions, Geophys. Res. Lett., 4, 311, 1977.

Mosier, S. R., and D. A. Gurnett, Observed correlations between auroral and VLF emissions, J. Geophys. Res., 77, 1137, 1972.

Mozer, F. S., C. W. Carlson, M. K. Hudson, R. B. Torbert, B. Parady, T. Yatteau, and M. C. Kelley, Observations of paired electrostatic shocks in the polar magnetosphere, Phys. Rev. Letters, 38, 292, 1977.

Potemra, T. A., Large-scale characteristics of field-aligned currents determined from the Triad magnetometer experiment, in Dynamical and Chemical Coupling of Neutral and Ionized Atmosphere, B. Grandel, ed., D. Reidel, Dordrecht-Holland, in press 1977.

Sharp, R. D., R. G. Johnson, and E. G. Shelley, Observation of an ionospheric acceleration mechanism producing energetic (keV) ions primarily normal to the geomagnetic field direction, J. Geophys. Res., 82, 3324, 1977.

Shelley, E. G., R. D. Sharp, and R. G. Johnson, Satellite observations of an ionospheric acceleration mechanism, Geophys. Res. Lett., 3, 654, 1976.

Torbert, R. B., and Mozer, F. S., Electrostatic shocks as the source of discrete auroral arcs, Geophys. Res. Letters, in press 1978.

Figure Captions

Fig. 1. Histogram distribution of the average probability of observation of an upward flowing ion event in the altitude range from 6000-8000 km as a function of invariant latitude for H^+ and O^+ ions in the energy range 0.5 to 16 keV. Error bars indicate statistical uncertainty.

Fig. 2. Comparison of auroral frequency distribution at solar minimum (Feldstein et. al., 1969) with the distribution of upward flowing ion events.

Fig. 3. Relative probability of occurrence of an upward-flowing ion event as a function of magnetic local time for the altitude range from 6000-8000 km. The distribution was normalized to one at its maximum value.

Fig. 4(a). Average probability of observing an upward flowing ion event as a function of altitude. (b). Differential probability of occurrence as a function of altitude derived from Figure 4(a). Values were renormalized to yield an integral probability of one.

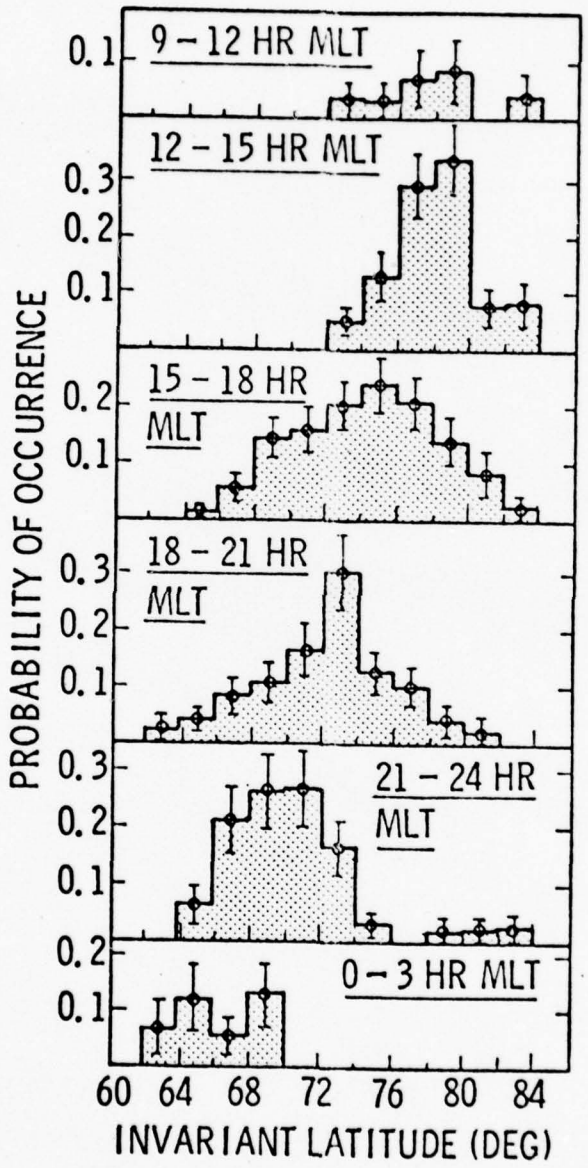
9 – 12 HR MLT
12 – 15 HR MLT
15 – 18 HR MLT
18 – 21 HR MLT
21 – 24 HR MLT
0 – 3 HR MLT
PROBABILITY OF OCCURRENCE
0.1
0.3
0.2
0.1
0.2
0.1
0.3
0.2
0.1
0.3
0.2
0.1
0.2
0.1
60 64 68 72 76 80 84
INVARIANT LATITUDE (DEG)

FIGURE 1

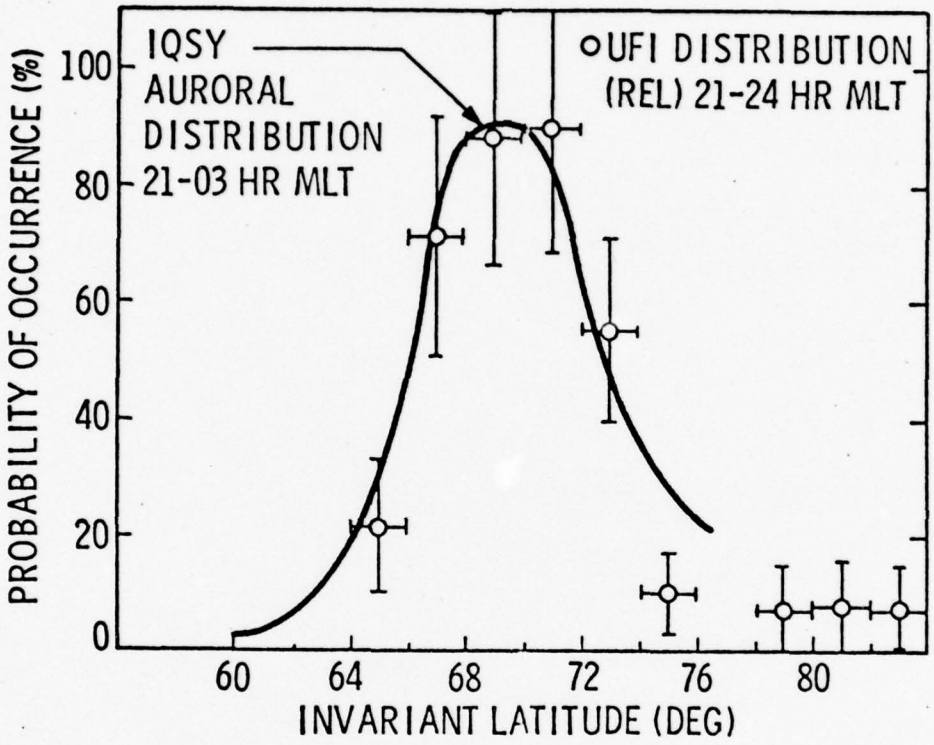
IQSY
AURORAL
DISTRIBUTION
21-03 HR MLT
UFI DISTRIBUTION
(REL) 21-24 HR MLT
PROBABILITY OF OCCURRENCE (%)
100
80
60
40
20
0
60
64
68
72
76
80
INVARIANT LATITUDE (DEG)

FIGURE 2

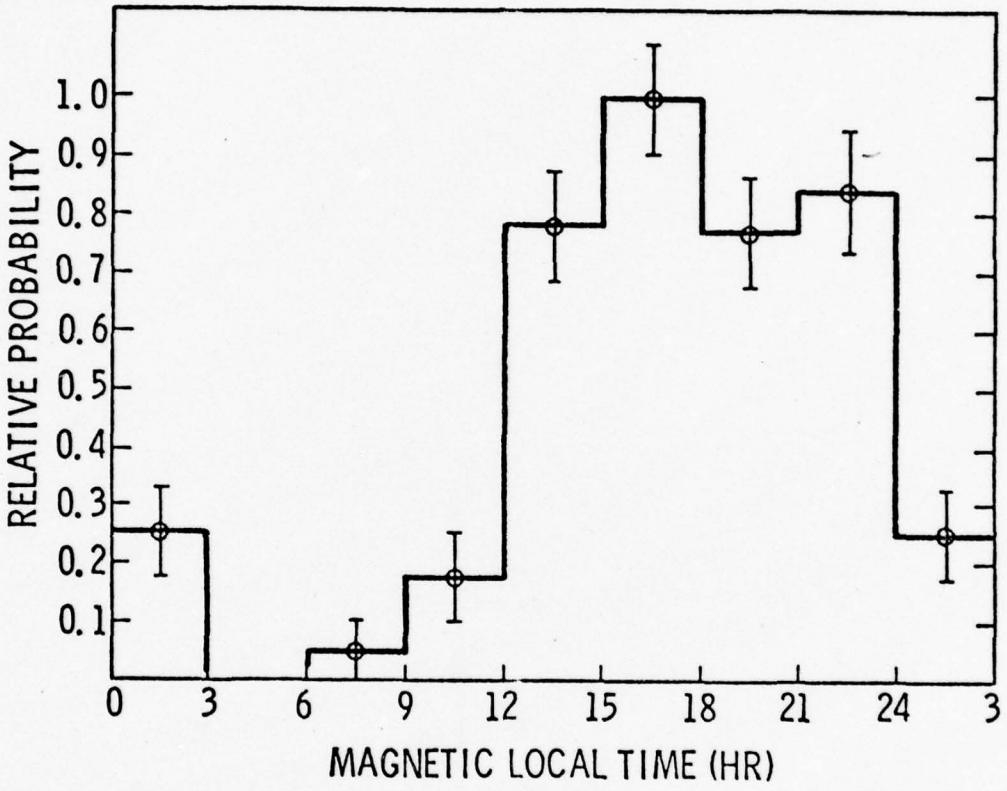
RELATIVE PROBABILITY
1.0
0.9
0.8
0.7
0.6
0.5
0.4
0.3
0.2
0.1
0
3
6
9
12
15
18
21
24
3
MAGNETIC LOCAL TIME (HR)

FIGURE 3

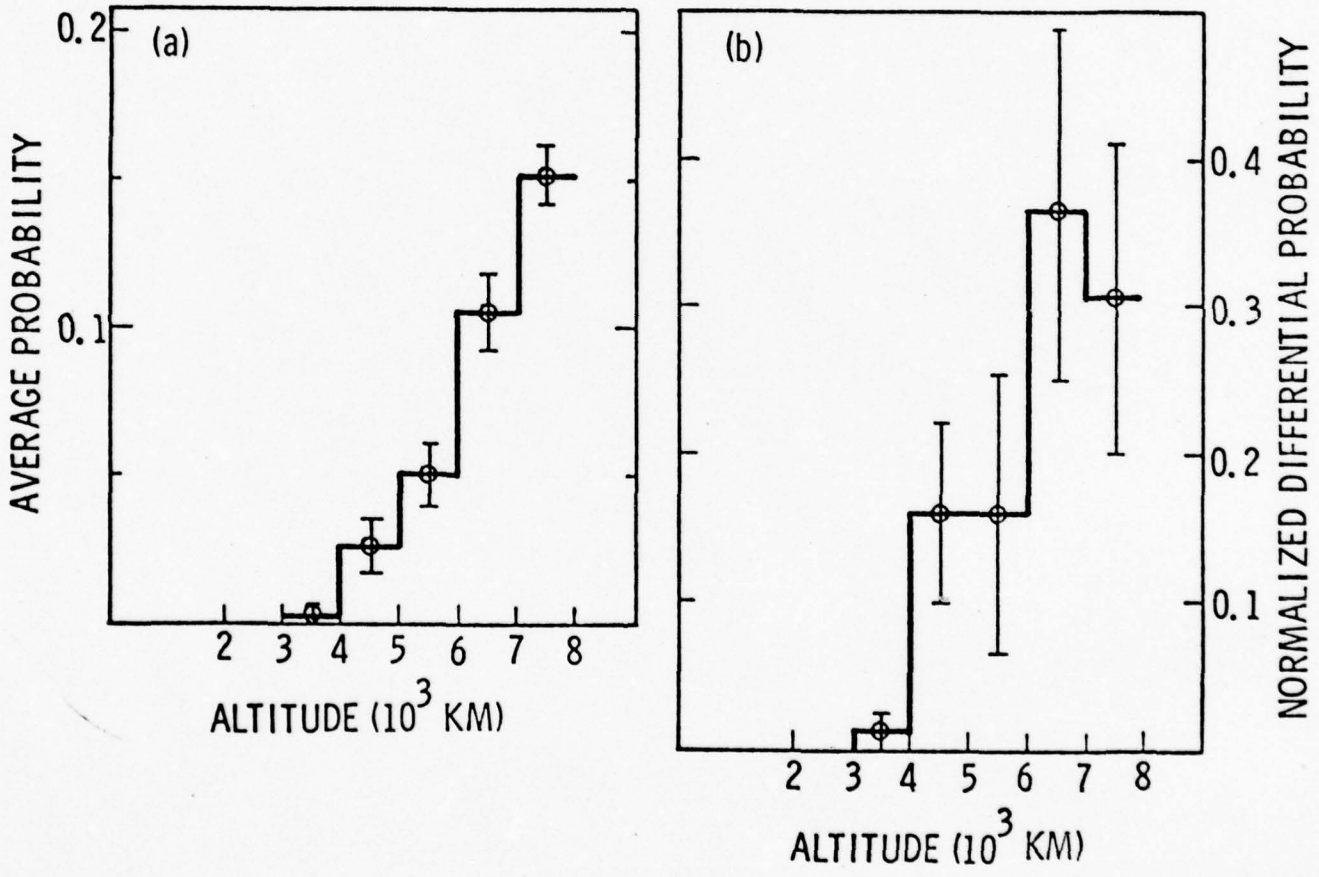
(a)
0.2
0.1
AVERAGE PROBABILITY
2 3 4 5 6 7 8
ALTITUDE (10^3 KM)
(b)
0.4
0.3
0.2
0.1
NORMALIZED DIFFERENTIAL PROBABILITY
2 3 4 5 6 7 8
ALTITUDE (10^3 KM)

FIGURE 4

ENERGETIC PARTICLE MEASUREMENTS FROM WITHIN IONOSPHERIC STRUCTURES RESPONSIBLE FOR AURORAL ACCELERATION PROCESSES

R. D. Sharp, R. G. Johnson, and E. G. Shelley
Lockheed Palo Alto Research Laboratory
3251 Hanover Street
Palo Alto, California 94304

March 1978

ABSTRACT

Measurements of energetic electrons ($0.07 \leq E \leq 24$ keV) and ions ($0.5 \leq E \leq 16$ keV) on the S3-3 satellite show features which are interpreted in terms of parallel potential drops of up to several kV magnitude existing simultaneously both above and below the satellite. This leads to the inference that the satellite is within an auroral acceleration region. Two events of this type are examined in which the satellite is in the 7000-8000 km altitude range and at auroral latitudes. Both events are interpreted as traversals of an "inverted V" acceleration region of broad latitudinal width (2° - 4°). In both cases, one can infer a vertical extent to the acceleration region of $\gtrsim 10^3$ km.

I. INTRODUCTION

Previous results have suggested that at least some types of auroral electron acceleration processes occur within large scale ionospheric structures containing potential drops of the order of 10^4 eV aligned parallel to the magnetic field and situated at altitudes above those which have been repeatedly sampled by experiments on rockets and low altitude, polar-orbiting satellites [Gurnett, 1972; Evans, 1974; Swift, 1975; Kauffman et al., 1976, Falthammer, 1977].

The S3-3 satellite (8,000 km apogee, 240 km perigee, 97.5° inclination) is now sampling this region of the magnetosphere and has discovered that such structures are indeed a commonly occurring phenomena at altitudes of about 1 R_E at auroral latitudes. Some of the manifestations of these phenomena are:

1. Upward flowing, narrowly collimated beams of energetic (keV) field aligned ions, indicative of electrostatic acceleration of ambient ionospheric ions. [Shelley et al., 1976, Ghielmetti et al., 1978]

2. Occasional conical pitch angle distributions in the energetic ions indicating additional processes providing a perpendicular as well as a parallel component to the ion acceleration. [Sharp et al., 1977; Ghielmetti et al., 1978].

3. Signatures of keV potential drops both above and below the satellite in the energetic electron populations [Mizera and Fennell, 1977; Cladis and Sharp, 1977a, b].

4. Narrow spatial regions with measured d.c. electric fields $\gtrsim$ 10^2 mV/m which are referred to as electrostatic shocks by the Berkeley experiment/ers [Mozer et al., 1977; Torbert and Mozer, 1978].

In this paper we show some examples of the plasma observations from within these ionospheric structures, focusing primarily on the use of the electron pitch angle distributions as a diagnostic tool to probe for indicators of their geometry, particularly their vertical extent. A detailed discussion of the use of this type of analysis on another event has been presented by Cladis et al. [1977].

The Lockheed experiment on S3-3 consists of three ion-mass-spectrometers and four magnetic electron spectrometers which have been described in previous publications [Shelley et al., 1976, Sharp et al., 1977]. The satellite is spinning at approximately 3 rpm with its spin axis perpendicular to the orbital plane and the instruments are mounted with their view directions perpendicular to the spin axis, providing almost complete pitch angle scans of the measured fluxes. The angular acceptance range for the spectrometers is approximately 6° full width. The electron spectrometers have broad energy bands and nearly rectangular response functions so as to include almost all electrons with $.07 \leq E \leq 24$ keV in the four measured intervals (See Table I). They are sampled twice per second providing approximately 9° angular resolution. The ion spectrometers each have 4 energy-per-charge settings which are stepped every 16 seconds. These are also listed in Table I. The ion spectrometers provide a complete mass-per-charge sweep at each of three energy-per-charge values every 1 second.

Since the satellite spins at $\sim$3 rpm and it requires several spins to be able to differentiate characteristic pitch angle structure from spatial or temporal variations, we focus these studies on ionospheric structures with a broad latitudinal extent which, as we will see, are inferred to have relatively weak parallel electric fields (of the order of millivolts per meter) extending over vertical dimensions of $\sim 10^3$ km. These are possibly a different class of phenomena than those being studied by the Berkeley group [Mozer et al., 1977] whose experiment more naturally focuses on high electric field phenomena

($\sim 10^2$ mv/m) which are found to occur over narrow ($\lesssim$ few km) latitudinal dimensions[Torbert and Mozer 1978]. The two classes of phenomena are generally associated spatially but are not identical. An example of this spatial association is given in Figure 1 which shows data obtained over the northern hemisphere auroral zone on 29 July 1976. The abscissa shows universal time, altitude in kilometers, invariant latitude, magnetic local time, and L value. The four lowest panels show the logarithm of the counts per half-second counting interval for the electron spectrometers. The panel labeled PITCH shows the pitch angle of the look direction of the spectrometer. The next four panels show the logarithm of the counts from ions with m/q = 1,2,4, and 16, respectively, summed once per second from selected output channels from all three of the mass spectrometers giving an approximate measure of the relative flux of the relevant species. The top panel shows the energy step of each of the three mass spectrometers. The spin numbers are labeled for reference. For example, for the 16-second period associated with spin 12 the three spectrometers were set at E/q values of 1.28, 4.5, and 16.0 keV, respectively, and the m/q = 1 plot shows the sum of the proton counts at these three energies. In fact, on this spin the observed counts derived almost entirely from the high energy spectrometer indicating a peak in the spectrum at $E \gtrsim 16$ keV.

In examining Figure 1 one sees two regions, labeled Region I and Region II, each of which contains particle fluxes with common signatures extending over a wide latitudinal range. Region I shows symmetric, 90° peaked pitch angle distributions in the three lowest energy electron channels which, as will be shown, are indicative of a broad region of parallel electric fields located above the spacecraft. Region II is a broad region of upward flowing ions associated with a drop-out in the low energy electron fluxes which is indicative of a potential drop below the spacecraft.

Both of these regions are contained within a larger scale region in which the electron fluxes, as measured by the Aerospace Corporation's electrostatic analyzers, show the characteristic signature of an "inverted V" event

when plotted on a grey scale energy-time spectrogram. [Mizera and Fennell, 1978; the spectrogram for this event is shown in Figure 3 of this reference.] Within this large scale "inverted V" region four discrete, narrow, electrostatic shocks have been reported by the Berkeley group [Mozer et al., 1977] at the locations indicated on the lowest horizontal axis in Figure 1. Upward flowing energetic ions are occasionally observed at the locations of the electrostatic shocks [Mizera et al., 1977] when the plasma analyzers are fortuitously oriented downward at the times of passage through the narrow structures. On this occasion the Lockheed spectrometers saw no upward flowing ions until the satellite reached Region II.

As indicated above, this report will focus on the broad scale structures. Preliminary indications are that these regions are generally spatially associated with enhanced low frequency noise or turbulence in the electric field data [Torbert and Mozer, 1978]. The signatures of the parallel potential drops within the structures consist of the upward flowing ion beams plus certain features of the electron pitch angle distributions to be described below. Signatures of potential drops above and below the satellite are often observed simultaneously indicating a substantial vertical extent to the structures. As discussed by Ghielmetti et al. [1978] the ion beams often show the combined effects of perpendicular and parallel accelerations as well as the transfer of energy between the two components by the mirroring action of the magnetic field. This complication plus the time lags in the ion data due to the substantial times of flight involved (e.g., 1 keV O^+ ions require over 9 secs to travel 1000 km) make the ion data less useful for quantitative analysis in possibly time-varying events than the rapidly moving electrons. Therefore, in these initial studies we will focus on the electron signatures.

For the following discussion we define primary electrons as those electrons entering the acceleration region from above and those electrons which have passed through the acceleration region and are reflected below the spacecraft before interacting with the atmosphere. We define degraded primary electrons as those primary electrons which have lost energy in the atmosphere below the acceleration region, and we define secondary electrons as those electrons which have been produced in the atmosphere below the acceleration region by the primary electrons. As illustrated in Figure 2, the electrons observed in the presence of a parallel upward-directed electric field above the spacecraft fall into two general categories; primaries and degraded primaries with energy greater than the potential drop above the spacecraft, ($E > \phi_A$), and secondaries and degraded primaries with energy less than the potential drop ($E < \phi_A$). The latter class is characterized by an up-down symmetry in their pitch angle distributions since the upcoming electrons from the atmosphere are all reflected by ϕ_A. Since the primary electrons are all accelerated to energies greater than ϕ_A, a detector whose energy band is entirely below ϕ_A will shown an up-down symmetry as indicated in Figure 2a. In addition to the short-lived particles topologically connected to the atmosphere (shaded region in Figure 2a), one often sees a quasi-stable component of the fluxes in this energy range which are trapped between the magnetic mirror below the spacecraft and the electric mirror above (angular regions indicated by circles in Figure 2a). This population is fed by scattering and by fluctuations in the electric fields and, because of intensity fluctuations in the flux levels of the primaries, can build up to levels greater than the instantaneous levels observed in the loss cone. Examples of this class of signatures are the Region I electron fluxes in CMEA, CMEB, and CMEC shown in Figure 1 and the CMEA fluxes in the central portion of the event illustrated in Figure 7.

The electrons with $E > \phi_A$, generally exhibit a well-defined loss cone which destroys the up-down symmetry and establishes their identification. The loss cone is both widened and deepened by the potential below the spacecraft [Cladis et al., 1977] with the widening simply related to the magnitude of this potential through the expression:

$$\sin^2 \alpha_L = \frac{B_S}{B_T} \quad \frac{E_S + \phi_B}{E_S} \tag{1}$$

where α_L is the angular half width of the loss cone. ϕ_B is the kinetic energy gained in the parallel field below the satellite, B_S and B_T are the magnitudes of the magnetic field at the location of the satellite and the top of the atmosphere respectively, and E_S is the measured energy of the electrons at the location of the satellite.

The primary electrons with energies only moderately greater than ϕ_A also exhibit an angular cutoff in the vicinity of 90°. This can be interpreted as a result of the action of the first adiabatic invariant:

$$\sin^2 \alpha_C = \frac{B_S}{B_1} \cdot \frac{E_S - \phi_A}{E_S} \tag{2}$$

where α_C is the angular location of the cutoff, ϕ_A is the kinetic energy gained in the parallel field between the satellite altitude and Z_1 (see Figure 2) and B_1 is the magnetic field strength at Z_1. This equation has two quantities which are generally unknowns, ϕ_A and B_1. B_1 is of particular interest since it is related to the vertical scale size of the ionospheric structure (labeled d in Figure 2) which can serve to help differentiate between various models for the cause of the parallel potential drops (e.g., double layers, oblique shocks, anomalous resistivity) which have character-

istically different scale sizes. In this work we will assume isotropy of the incident spectrum (for $Z > Z_1$) and utilize simultaneous measurements of electrons in the different energy ranges to provide information on both unknowns in Equation (2) thereby inferring values for the parameter d , as well as obtaining estimates of ϕ_A and ϕ_B from the measured cutoffs in the pitch angle distributions at α_C and α_L.

Since we are utilizing broad band electron detectors some uncertainty arises in the assignment of E_S in these expressions for α_C and α_L. To improve the accuracy of the estimates of ϕ_A, ϕ_B, and d one can fit an assumed distribution function to the detector response or otherwise use supplementary information from other detectors. We have taken this approach to estimate the energy E_S to be associated with the pitch angle α_C corresponding to 50% of the total reduction in the count rate in the region of the angular cutoff.

A more general and extended discussion of these and other signatures of parallel electric fields in the particle distribution functions has been presented by Kauffman et al. [1976], and Whipple [1977].

II. JULY 29, 1976, 11:28 UT EVENT

As discussed above, the up-down symmetry in the pitch angle distributions in CMEA, CMEB, and CMEC in Region I indicates that they are responding primarily to electrons with energies $< \phi_A$. This implies that the primary electrons are accelerated out of the detector's energy range and establishes a lower limit of $\phi_A \gtrsim 5$ keV in this region. CMED which is responding to the primary portion of the electron spectrum shows the 90° minimums in the pitch angle distributions expected to result from ϕ_A as discussed in Section I. The transition from 90° maximum to 90° minimum type pitch

angle distributions evidently occurs in the lower end of the CMED energy window since the observed 90° minimums are occasionally somewhat obscured by electrons which retain the 90° peaked angular distributions characteristic of the lower energy channels (see Figure 1). The CMED pitch angle distribution for spin 3+ (i.e., the second of the two pitch angle scans on spin 3) is illustrated in expanded form as the upper curve of Figure 3. The average value of α_C as defined above for this distribution is 63°. In order to attempt to determine the uncertainty introduced by the contribution from the 90° peaked low energy electrons, we note from Figure 1 that the shape of the 90° maxima in the angular distributions is generally not a strong function of energy. This is illustrated in more detail for spin 3+ in Figure 4. We therefore subtract a quantity with the shape of the measured CMEC pitch angle distribution from the CMED distribution in Figure 3 in order to evaluate the uncertainty such a contribution might introduce to the estimated value of α_C. The maximum magnitude such a contribution could have is that required to reduce the measured CMED 90° flux to zero. The residual CMED flux after the subtraction of such a distribution is illustrated by the dashed curve in Figure 3. A similar curve corrected for a 90° peaked contribution of half this magnitude is illustrated by the dotted curve. Both the dotted and dashed distributions yield average α_C values of 63° equivalent to that derived from the uncorrected (solid) curve. Thus the measured value of this quantity is insensitive in this case to the magnitude of the correction and can be used to estimate B_1 from Equation (2) and the parameter d as discussed in Section I.

Within the range of the CMED detector the electron flux during this period is generally decreasing with increasing energy [P. F. Mizera, private communication] and the midpoint of the energy band (15.4 keV) can be taken

as an upper limit on E_S. Using the lower limit of 5 keV on ϕ_A derived from the CMEC pitch angle distribution, we obtain $B_S/B_1 \gtrsim 1.2$ and $d \gtrsim 800$ km assuming a $1/r^3$ magnetic field dependence.

An alternative lower limit can be obtained provided there is some residual primary flux at 90° within the bandpass of the detector which has not been excluded by the action of ϕ_A (for example one of the two upper curves in Figure 3). In these circumstances, electrons with energies at least as low as the upper end of the CMED energy window (23.5 keV) can reach $\alpha \geq 90°$ at the satellite altitude. Thus in Equation (2) we can set $\alpha_C = 90°$ and $E_S \leq 23.5$ keV for a limit on $B_S/B_1 \gtrsim 1.3$ and $d \gtrsim 1100$ km.

The parallel potential drop below the spacecraft in region I is of relatively low magnitude. The width of the CMED loss cone ($\alpha_L = 19°$) shown for spin 3+ in Figure 3 is equal to its expected value in the absence of such a potential. No upward-flowing ions (with E > 0.5 keV) were observed in the Lockheed mass spectrometers. The Aerospace electrostatic analyzers did in fact see weak upstreaming ion fluxes in the 100 eV range. [Mizera and Fennell, 1978] so a weak potential probably did exist below the spacecraft, but its magnitude was too low to be detected with the techniques utilized here.

Region II on the other hand is characterized by the signatures of a large ϕ_B. As discussed in Section I, one sees continuous upstreaming ion beams with energies up to 16 keV. The electron loss cones are also significantly widened with respect to Region I (see Figure 1). This is illustrated for spin 7+ in more detail in Figure 5 where for CMED $\alpha_L = 28°$ corresponding to a $\phi_B \simeq 13$ keV.

Another indicator of the strong ϕ_B in Region II is the dramatic suppression of the low energy secondary and degraded primary electrons in this region relative to Region I. A potential drop above the spacecraft is also

implied by this signature since the primary spectrum is accelerated to higher energies, but in general this is not sufficient to suppress the low energy electron fluxes since, depending on the primary spectrum, the fluxes of upcoming and reflected secondaries in a given low energy region can exceed the fluxes of primaries that existed in that region prior to the onset of the ϕ_A. The ϕ_B on the other hand acts both to reflect the lowest energy secondaries and reduce the level of the degraded primaries by the factor $E_S/(E_S + \phi_B)$ relating the flux at the top of the atmosphere to the flux at the satellite which enters through Liouville's theorem.

In contrast to the potential below the spacecraft, the potential above the spacecraft has not changed substantially between Region I and Region II. Even though the magnitude of the low energy secondaries and degraded primary electrons is suppressed, when detectable (i.e., in CMEC) they still exhibit the up-down symmetry characteristic of $\phi_A \gtrsim 5$ keV (see Figure 6). (Later, toward the end of Region II [$\sim$spin 12] one sees in CMEC the transition to a loss cone/antiloss cone asymmetry indicating that ϕ_A is decreasing to the CMEC energy range [see Figure 1].) The CMED distribution for spin 7+ illustrated in Figure 5 shows a 90° minimum with $\alpha_C = 62°$, about the same as in spin 3+, again approximately independent of a correction for a low energy component peaked at 90°. From the Aerospace spectrogram (op. cit.) one finds that the energy spectrum of the primary electrons in this period has not deviated appreciably from Region I. Thus we can conclude that the electric field geometry above the spacecraft is approximately the same as in Region I (d extending to $\gtrsim 10^3$ km) but that the field below the spacecraft has dramatically increased.

III. SEPTEMBER 15, 1976, 1058 UT EVENT

The July 29 event described in Section II was selected primarily to illustrate the relationship of the broad parallel electric field regions to the electrostatic shock regions observed by Mozer et al. [1977]. It was a relatively complicated event with overall potential drops of larger magnitude than are typical. In this section we will describe a simpler, less intense, and isolated event with a quasi-symmetric structure that allows for separation of spatial and temporal variations which generally are indistinguishable in measurements from a single satellite. Survey plots for this event are shown in Figure 7 in a format similar to Figure 1. One sees significant fluxes of upflowing ions and substantially widened loss cones in CMEB in the central portion of the event (spins 2, 3, and 4) indicative of a potential drop below the spacecraft. The maximum energy at which the upstreaming ion fluxes were observed was 1.76 keV on spin 3. In this same region one sees 90° peaked pitch angle distributions with an up-down symmetry in CMEA similar to those found in the low energy channels in the July 29 event. There are also 90° minimums in the CMEB distributions which are most obvious in the wings of the event, outside the region of the 90° maximums in the lower energy electrons. Narrowly collimated, field-aligned, downward-flowing electron "spikes" are seen at the edges of the event in CMEA. This is a commonly observed signature in this channel at the edges of the ionospheric structures. We interpret these data to indicate that there is a field-aligned potential drop above the spacecraft throughout the event, with weak ϕ_A at the edges of the event where CMEA is responding to primary electrons in the field-aligned spikes; and an increasing ϕ_A toward the center of the event where the depression in the CMEA flux levels and their up-down symmetry implies that $\phi_A \gtrsim .24$ keV.

The symmetric nature of the ionospheric structure in this event is best illustrated by intercomparing the pitch angle distributions at the high and low latitude edges of the event by "folding" Figure 7 so that the two CMEA spikes are superimposed. This has been done in Figure 8 where both the CMEA and CMEB responses are shown plotted versus pitch angle rather than time in order to provide a more precise intercomparison. As indicated in the figure, time progresses from left to right for the data from the high latitude edge of the structure and from right to left for the data from the low latitude edge. The remarkable correspondence indicates that we are traversing a temporally stable structure and that the observed variations are primarily spatial and angular. It also suggests that there is some significance to this pattern at the edges of the structure in terms of the mechanism responsible for its origin.

A CMEB pitch angle distribution measured near the center of the event is shown in Figure 9. As in the previous example, the 90^{o} minimum is possibly somewhat obscured by a contribution from fluxes at the low end of the energy window with 90^{o} peaked distributions similar to those observed in CMEA. Again this seems plausible since it is unlikely that the transition from 90^{o} maximums to 90^{o} minimums in the pitch angle distributions occurs exactly at the edge of the energy window. Also, similar to the July 29 example, the uncertainty in α_C introduced by such a 90^{o} peaked contribution is small (see Figure 9). From the up-down symmetry of CMEA we can infer that all the primaries

have been accelerated out of its passband. This sets a lower limit on $\phi_A \gtrsim .24$ keV. The low response in CMEC suggests that the spectrum is falling in the CMEB energy range, so for a lower limit on the parameter d we use the midpoint of the CMEB energy band for E_S and obtain $d \gtrsim 1200$ km through the use of Equation 2.

As before an alternative limit can be obtained for models represented by the family of curves between the two extremes shown in Figure 10. For these cases, and for the upper curve, where there is a residual response at 90^o due to the assumed isotropic incident spectrum, one can set E_S in Equation 2 equal to the upper edge of the CMEB energy window (1.13 keV) and obtain a lower limit on B_S/B_1 corresponding to $d \gtrsim 1000$ km.

Burch et al. [1976] have found from measurements on a low altitude satellite beneath the electron acceleration regions in "inverted V" events that the electron distribution functions are well described by Maxwellian primary electron beams which have been accelerated through an electrostatic potential. A Maxwellian distribution has the property that acceleration through an electrostatic potential changes the magnitude but not the shape of the energy spectrum for energies greater than the value of the electrostatic potential. Thus under this assumption, the CMEB/CMEC response ratio R is a unique measure of the temperature of the Maxwellian, independent of ϕ_A, as long as ϕ_A is less than the lower edge of the CMEB energy window or .35 keV. As ϕ_A increases above this level it will depress this ratio since the primary electrons are excluded from the lower portion of the CMEB window. A plot of the CMEB/CMEC response ratio for this event is shown in Figure 10. The CMEB response was taken

at the peak of the pitch angle distribution on each spin while the CMEC response was averaged over the approximately isotropic region outside the loss cone. A plausible interpretation of these data is that the temperature is slowly varying throughout the event (except for the region of obvious hardening near spin 5+ associated with an increase in the CMEC response; see Figure 8) following the dotted curve in Figure 10. The depression in R from the dotted curve is then due to ϕ_A increasing above .35 keV. This interpretation is supported by the fact that we know from the depression in CMEA that ϕ_A is in fact increasing toward the center of the event, and by the approximate constancy in CMEC which would most likely be affected by a change in temperature. Under this interpretation, for spin 3+ we obtain ϕ_A = .54 keV from the measured depression in R.

The widest CMEB loss cone in this event, indicative of the maximum value of ϕ_B, occurred on spin 3+ and is shown in Figure 9. Using this α_L value and the E_S obtained from fitting the above described Maxwellian to the CMEB response function, we obtain ϕ_B = 1.9 keV from Equation 1. Thus the total parallel potential drop in this case is approximately 2.4 keV.

Another useful inference about the geometry of this event is obtained from the fact that the 90° minimums in CMEB are wider at the edges of the event (Figure 8) than in the center (Figure 9). We infer from the fact that the CMEA response has not yet fallen to the intensity level of the secondaries and degraded primaries that ϕ_A is less in these edge regions than in the central portion of the event. For a constant d , the 90° minimums should get narrower as ϕ_A gets smaller. Therefore d must be less at the edges than in the center.

IV. SUMMARY AND CONCLUSIONS

We have shown two examples of plasma measurements from within large scale ionospheric structures containing parallel electric fields. In the July 29, 1976 example there is an "inverted V" electron event of 4° latitudinal width within which there are two broad regions of parallel electric fields and a number of intense, narrow electrostatic shocks. Region I is inferred to have a parallel potential drop above the spacecraft of 5 kV or greater with a vertical dimension extending to $\gtrsim 10^3$ km above the spacecraft. Region II has a similar field geometry above the spacecraft and in addition shows evidence of a potential drop below the spacecraft of 13 kV or greater. In the September 15, 1976 example we infer: 1. A stable spatial structure of approximately 2° latitudinal width; 2. A vertical dimension extending to $> 10^3$ km above the spacecraft, larger in the center of the structure than at the edges; 3. A total field aligned potential drop of 2.4 kV with both ϕ_A and ϕ_B reaching their maximum values in the center of the structure. All of these features are qualitatively consistent with the V-shaped potential models proposed by Gurnett [1972], Swift [1975], and others to explain "inverted V" events.

The simultaneous observation of signatures of ϕ_A and ϕ_B implies that the electric fields involved extend over a large vertical dimension. If we assume that the fields determined from the inferred potentials and vertical scale sizes are continuous and roughly independent of altitude, we obtain field strengths of the order of $\sim$mV/m in these broad scale regions in contrast to the $\sim 10^2$ mV/m fields reported in the narrow electrostatic shocks [Mozer et al., 1977]. The inferred vertical scale sizes are much larger than characteristic dimensions such as the deBye length or the ion gyro radius;

however, this analysis cannot in fact differentiate between extended regions of low field and multiple double layers with regions of intense fields extending over short vertical dimensions situated both above and below the satellite.

ACKNOWLEDGMENTS

We thank J. B. Cladis for valuable discussions and P. F. Mizera and J. F. Fennell for providing unpublished data. This work was supported by the Atmospheric Sciences section of the National Science Foundation and the Office of Naval Research.

References

Burch, J. L., S. A. Fields, W. B. Hanson, R. A. Heelis, R. A. Hoffman, R. W. Janetzke, Characteristics of auroral electron acceleration regions observed by atmospheric explorer C, J. Geophys. Res., 81, 2223, 1976.

Cladis, J. B. and R. D. Sharp, Electrostatic potential differences along magnetic field lines inferred from satellite measurements of electron and ion distributions EOS, 58, 473, 1977a.

Cladis, J. B. and R. D. Sharp, Distribution of electrostatic potential along magnetic field inferred from observations of ion and electron fluxes, EOS 58, 716, 1977b.

Cladis, J. B., L. L. Newkirk, M. Walt, G. T. Davison, and W. E. Francis, Investigation of ionospheric disturbances, Report no. DNA-4225F, Defense Nuclear Agency, Washington, D.C. 20305, Jan. 28, 1977.

Evans, D. S., Precipitating electron fluxes formed by a magnetic field-aligned potential difference, J. Geophys. Res., 79, 2853, 1974.

Falthammer, C. G., Problems related to macroscopic electric fields in the magnetosphere, Rev. Geophys. and Space Phys., 15, 457, 1977.

Ghielmetti, A. G., R. G. Johnson, R. D. Sharp, and E. G. Shelley, The latitudinal, dirunal, and altitudinal distributions of upward flowing energetic ions of ionospheric origin, Geophys. Res. Lett., 5, 59, 1978.

Gurnett, D. A., Electric field and plasma observations in the magnetosphere in Critical problems of magnetospheric physics, edited by E. R. Dyer, IUCSTP Secretariat, National Academy of Sciences, Nov., 1972.

Kauffman, R. L., D. N. Walker, R. L. Arnoldy, Acceleration of auroral electrons in parallel electric fields, J. Geophys. Res., 81, 1673, 1976.

Mizera, P. F., J. F. Fennell, and A. L. Vampola, Charged particle distributions in the presence of large d.c. electric fields, EOS, 58, 472, 1977.

Mizera, P. F. and J. F. Fennell, quoted in Physics of heavy ions in the magnetosphere, by J. M. Cornwall and M. Schulz, in Solar system plasma physics, edited by C. F. Kennel, L. Lanzerotti, and E. Parker, North Holland Publ. Co., 1978 (in press).

Mizera, P. F., and J. F. Fennell, Signatures of electric fields from high and low altitude particle distributions, Geophys. Res. Lett., 4, 311, 1977.

Mozer, F. S., C. W. Carlson, M. K. Hudson, R. B. Torbert, B. Parady, T. Yatteau, and M. C. Kelley, Observations of paired electrostatic shocks in the polar magnetosphere, Phys. Rev. Letters, 38, 292, 1977.

Sharp, R. D., R. G. Johnson, and E. G. Shelley, Observation of an ionospheric acceleration mechanism producing energetic (keV) ions primarily normal to the geomagnetic field direction, J. Geophys. Res., 82, 3324, 1977.

Shelley, E. G., R. D. Sharp, and R. G. Johnson, Satellite observations of an ionospheric acceleration mechanism, Geophys. Res. Lett., 3, 654, 1976.

Swift, D. W., On the formation of auroral arcs and the acceleration of auroral electrons, J. Geophys. Res., 80, 2096, 1975.

Torbert, R. B., and Mozer, F. S., Electrostatic shocks as the source of discrete auroral arcs, Geophys. Res. Letters, in press 1978.

Whipple, E. D., Jr., The signature of parallel electric fields in a collisionless plasma, J. Geophys. Res., 82, 1525, 1977.

TABLE I. DETECTOR CHARACTERISTICS

DETECTOR	PARTICLE	ENERGY, keV	GDE, cm^2 s sr keV
CMEA	Electrons	0.07 - 0.24	1.2×10^{-6}
CMEB	Electrons	0.35 - 1.1	6.5×10^{-6}
CMEC	Electrons	1.6 - 5.0	1.9×10^{-5}
CMED	Electrons	7.3 - 24	6.5×10^{-5}

		Energy per unit charge			
		Step 1	2	3	4
CXA 1	Ions	0.50	0.68	0.94	1.28
CXA 2	Ions	1.76	2.4	3.3	4.5
CXA 3	Ions	6.2	8.5	11.6	16.0

FIGURE CAPTIONS

Figure 1 - Survey plots for July 29, 1976. Universal time (labeled SYST) is given on the abscissa. The location of four electrostatic shocks reported by Mozer el.al. (1977) are indicated by broad horizontal lines along the abscissa. The energy setting of the ion mass spectrometers (step number) is indicated at the top (see Table I.).

Figure 2 - Expected electron pitch angle distributions in the presence of a parallel electric field.

Figure 3 - CMED angular distribution on spin 3^+, July 29, 1976. See figure 1 for definition of spin numbers.

Figure 4 - CMEA, CMEB and CMEC angular distribution on spin 3^+, July 29, 1976.

Figure 5 - CMED angular distribution on spin 7^+, July 29, 1976.

Figure 6 - CMEC angular distribution on spin 7 and 8, July 29, 1976.

Figure 7 - Survey plots for September 15, 1976. Format is similar to figure 1.

Figure 8 - CMEA and CMEB angular distributions at the two edges of the acceleration region. The vertical arrows indicate the direction of motion of the measured electrons.

Figure 9 - CMEB angular distribution on spin 3^+, September 15, 1976. See figure 8 for definition of spin numbers.

Figure 10 - CMEB to CMEC response ratios over the acceleration region on September 15, 1976. The right hand ordinate shows the temperature of a Maxwellian determined by this ratio.

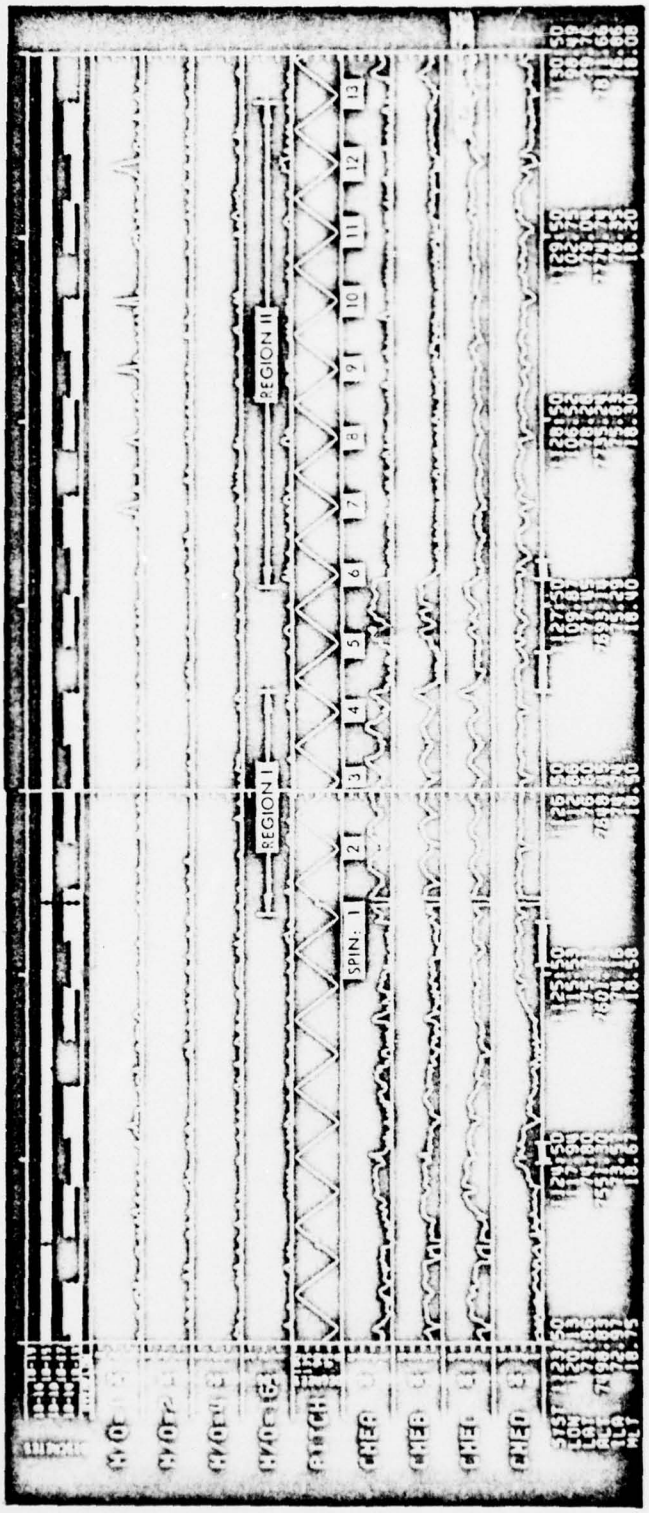

Figure 1

Figure 2

ELECTRON PITCH ANGLE DISTRIBUTIONS

SECONDARIES AND DEGRADED PRIMARIES, $E < \phi_A$

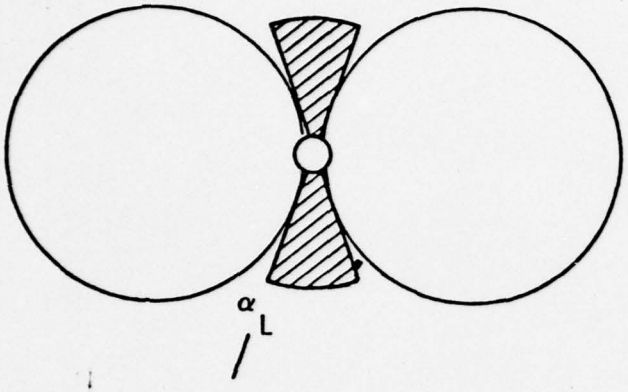

a.

PRIMARIES, $E > \phi_A$

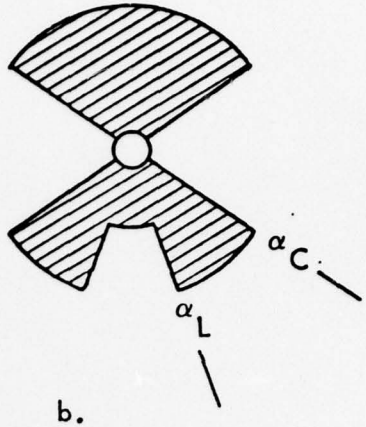

b.

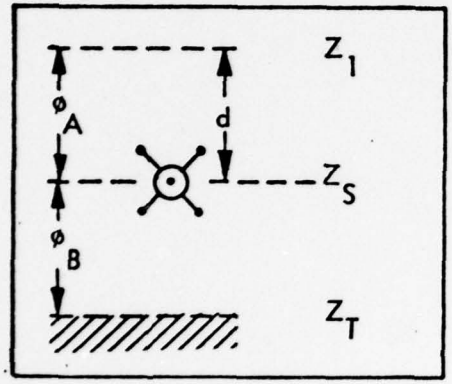

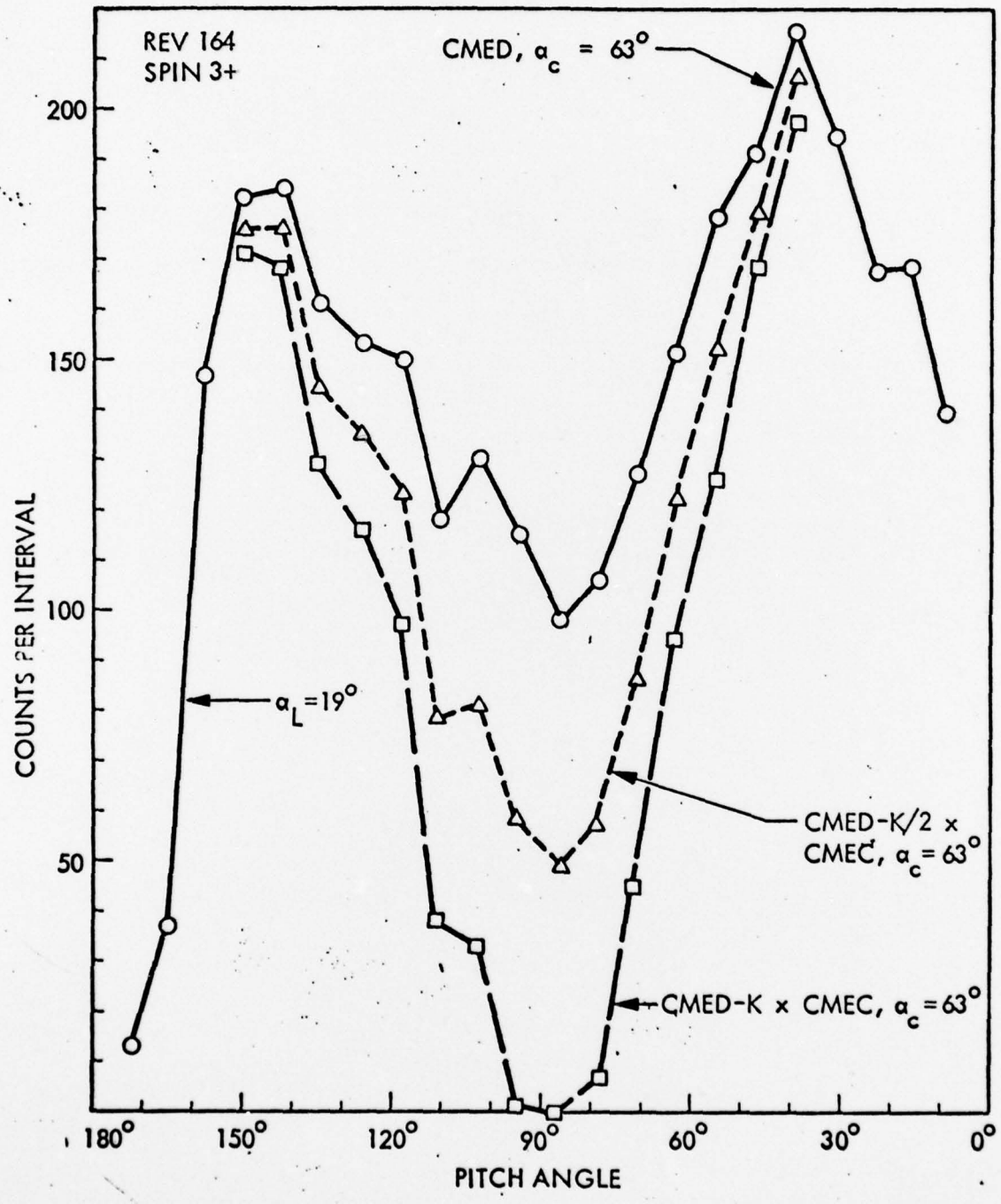
REV 164
SPIN 3+
CMED, α_c = 63°
200
150
100
50
COUNTS PER INTERVAL
α_L=19°
CMED-K/2 x CMEC, α_c=63°
CMED-K x CMEC, α_c=63°
180°
150°
120°
90°
60°
30°
0°
PITCH ANGLE

Figure 3

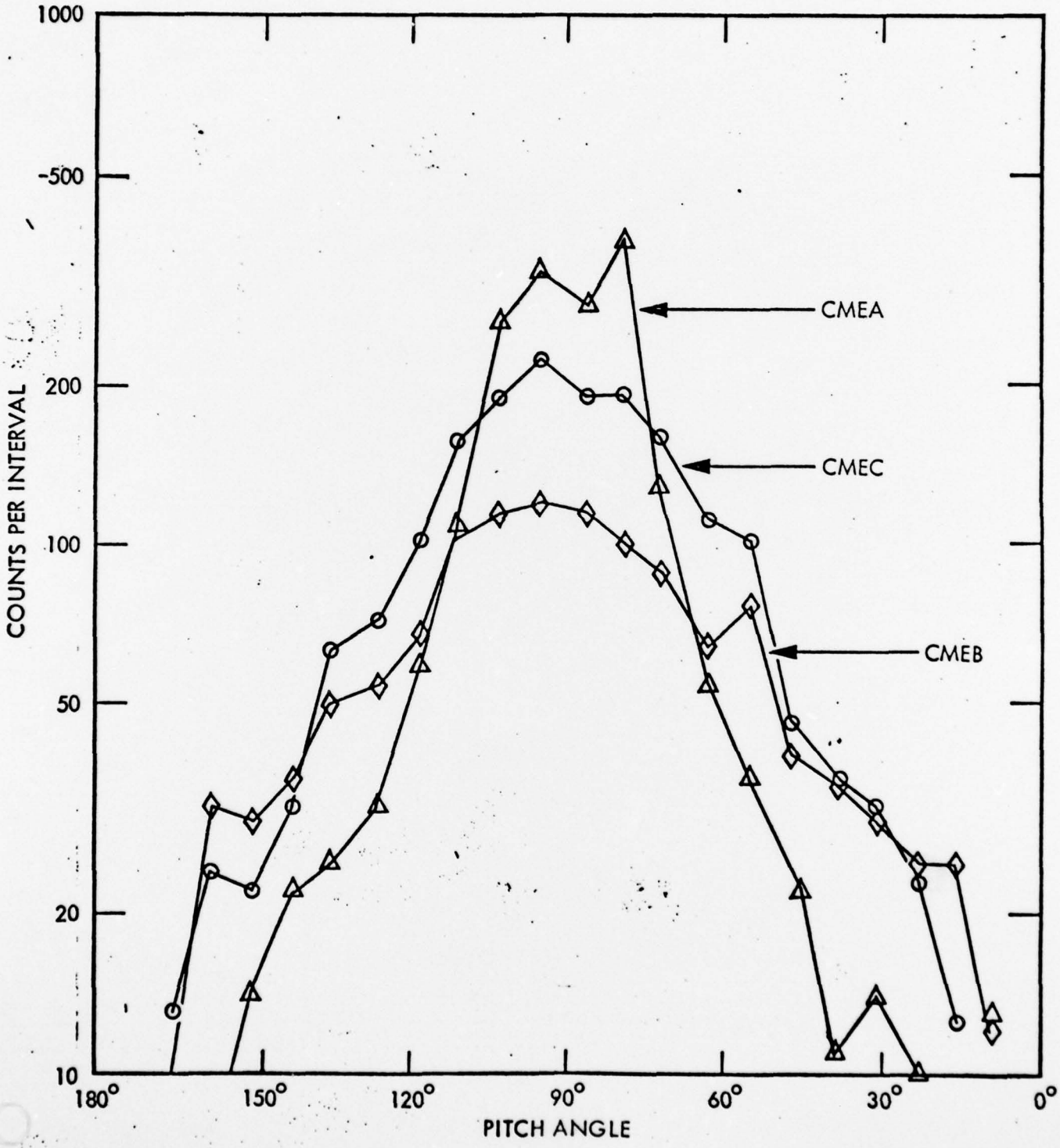
1000
-500
200
100
50
20
10
COUNTS PER INTERVAL
CMEA
CMEC
CMEB
180°
150°
120°
90°
60°
30°
0°
PITCH ANGLE

Figure 4

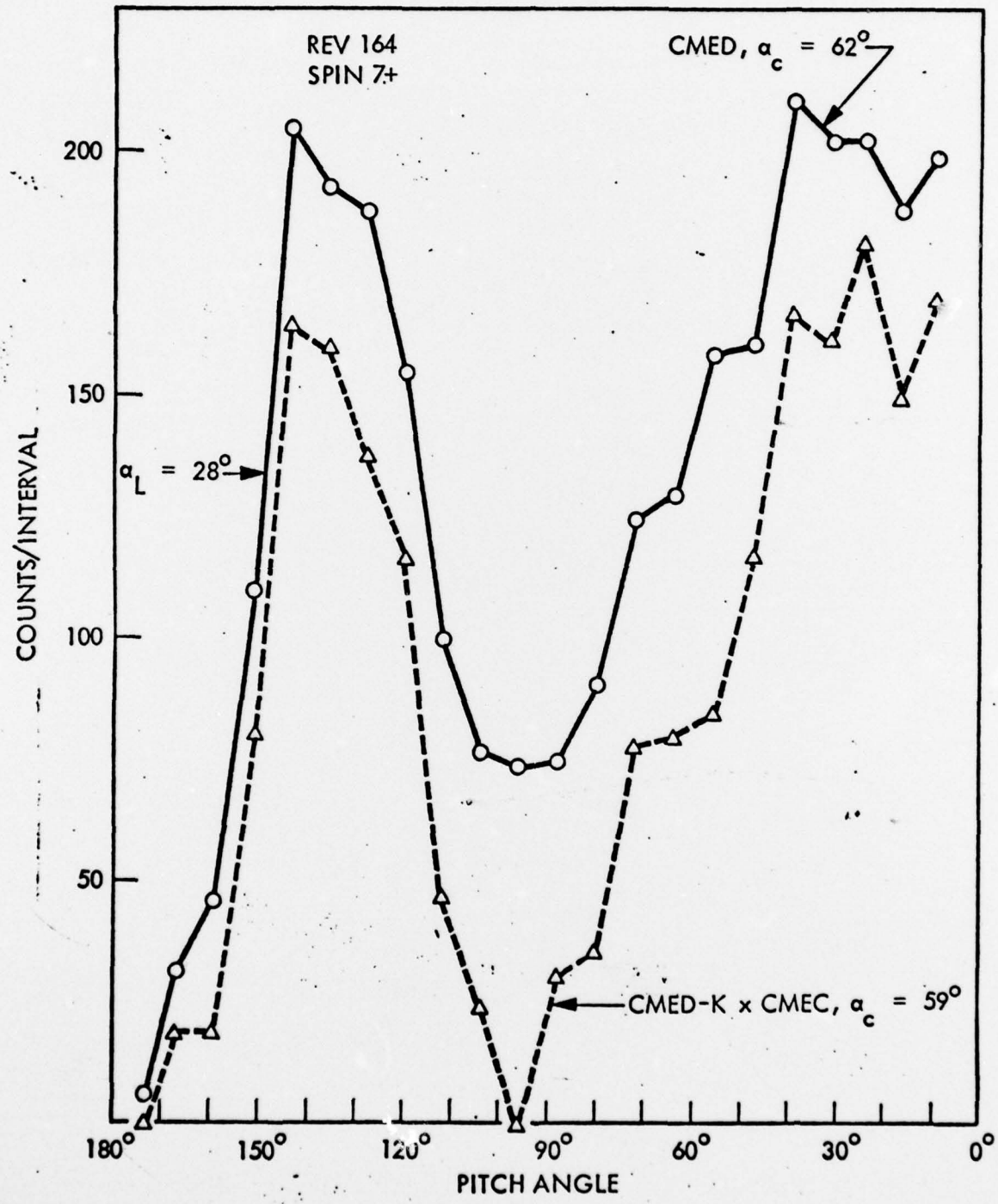
REV 164
SPIN 7+
CMED, α_c = 62°
200
150
100
50
COUNTS/INTERVAL
α_L = 28°
CMED-K x CMEC, α_c = 59°
180°
150°
120°
90°
60°
30°
0°
PITCH ANGLE

Figure 5

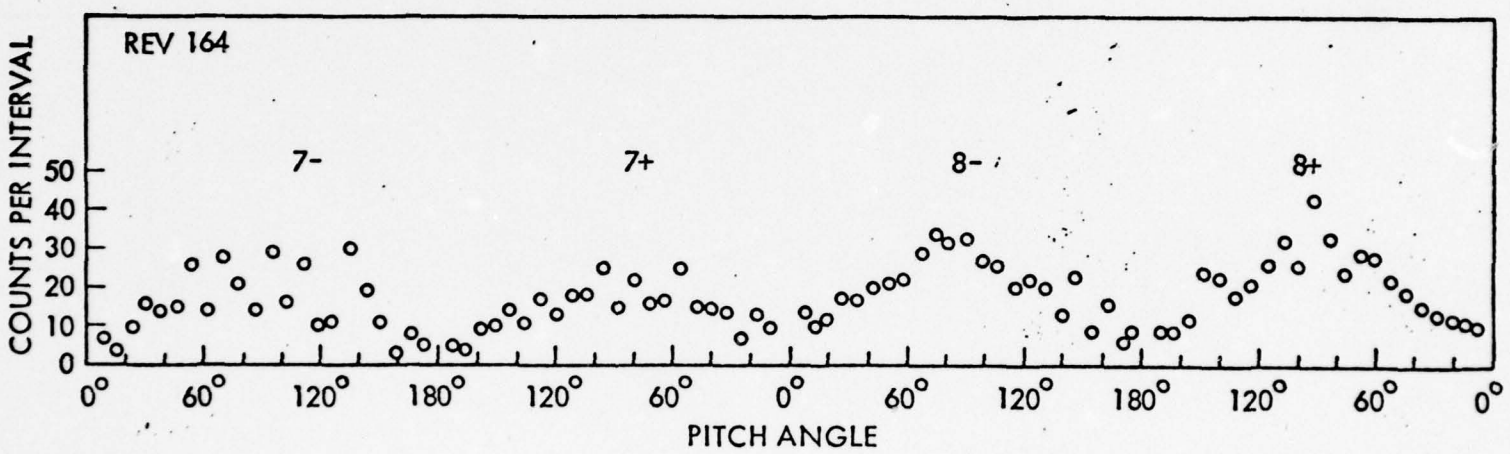
REV 164
7-
7+
8-
8+
COUNTS PER INTERVAL
0
10
20
30
40
50
0°
60°
120°
180°
120°
60°
0°
60°
120°
180°
120°
60°
0°
PITCH ANGLE

figure 6

Figure 7

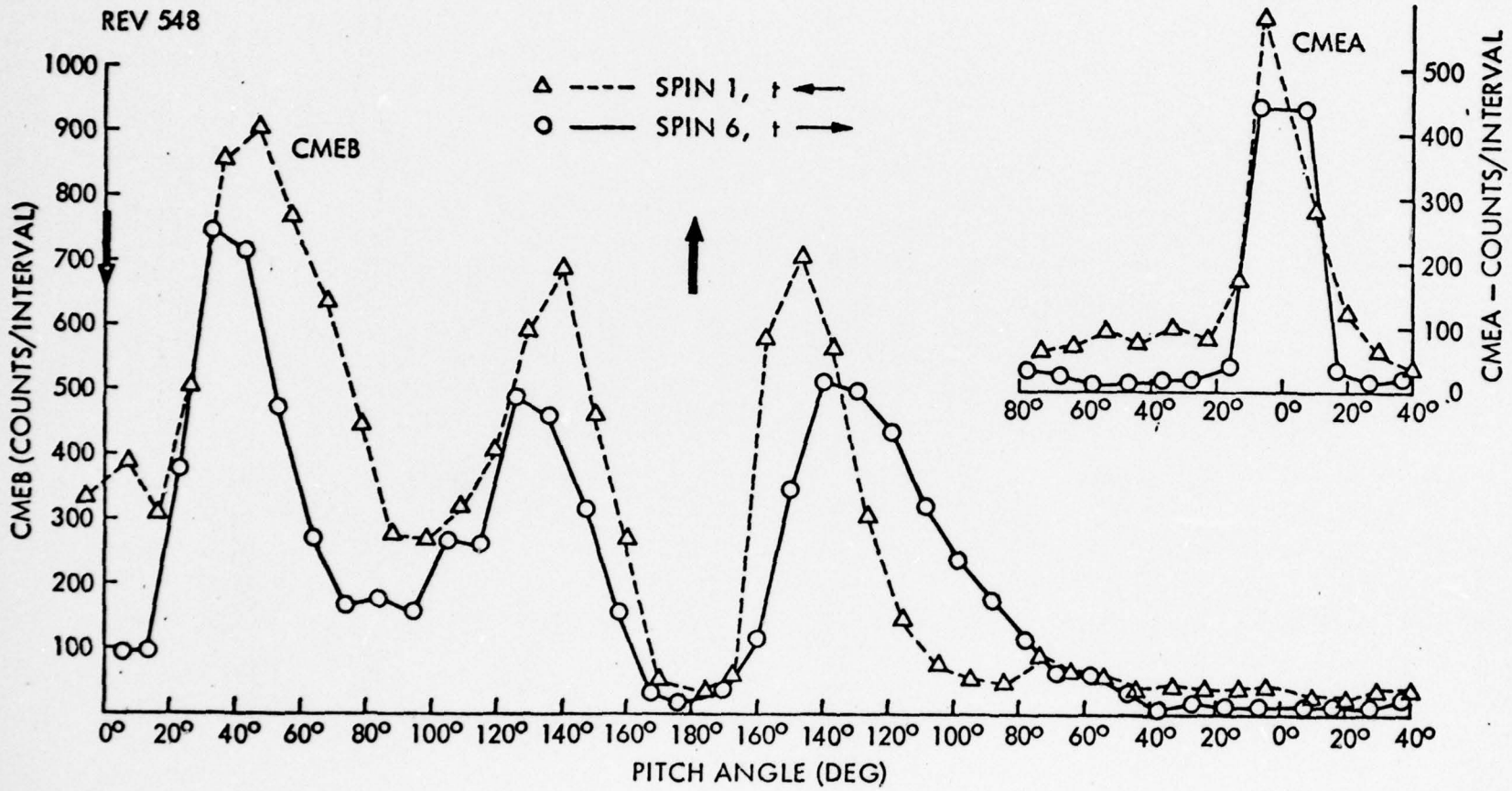
REV 548
CMEB
SPIN 1, t
SPIN 6, t
CMEA
CMEB (COUNTS/INTERVAL)
CMEA – COUNTS/INTERVAL
PITCH ANGLE (DEG)
1000
900
800
700
600
500
400
300
200
100
0
0° 20° 40° 60° 80° 100° 120° 140° 160° 180° 160° 140° 120° 100° 80° 60° 40° 20° 0° 20° 40°
80° 60° 40° 20° 0° 20° 40°

figure 8

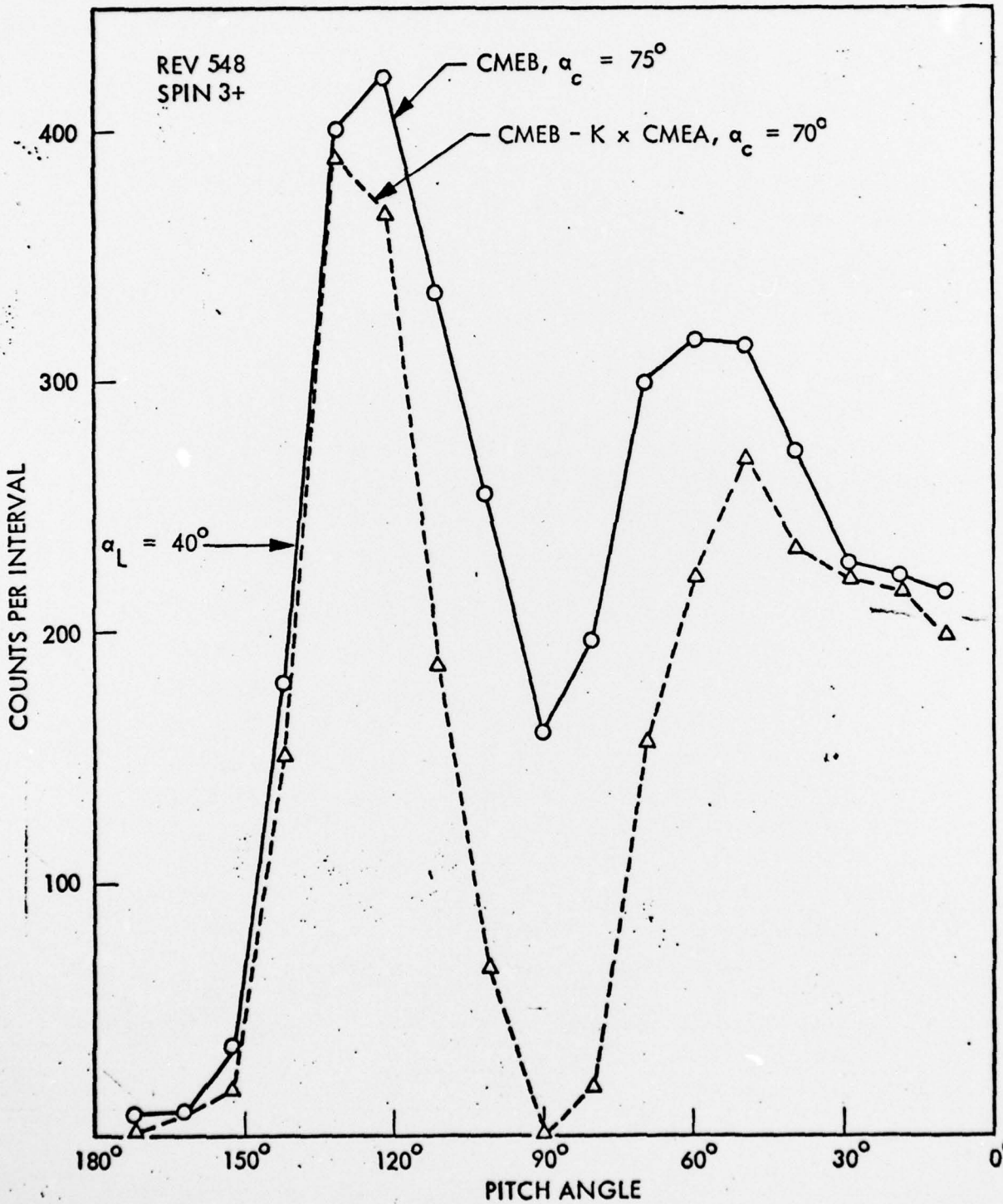
REV 548
SPIN 3+
CMEB, α_c = 75°
CMEB - K x CMEA, α_c = 70°
α_L = 40°
COUNTS PER INTERVAL
400
300
200
100
180°
150°
120°
90°
60°
30°
0°
PITCH ANGLE

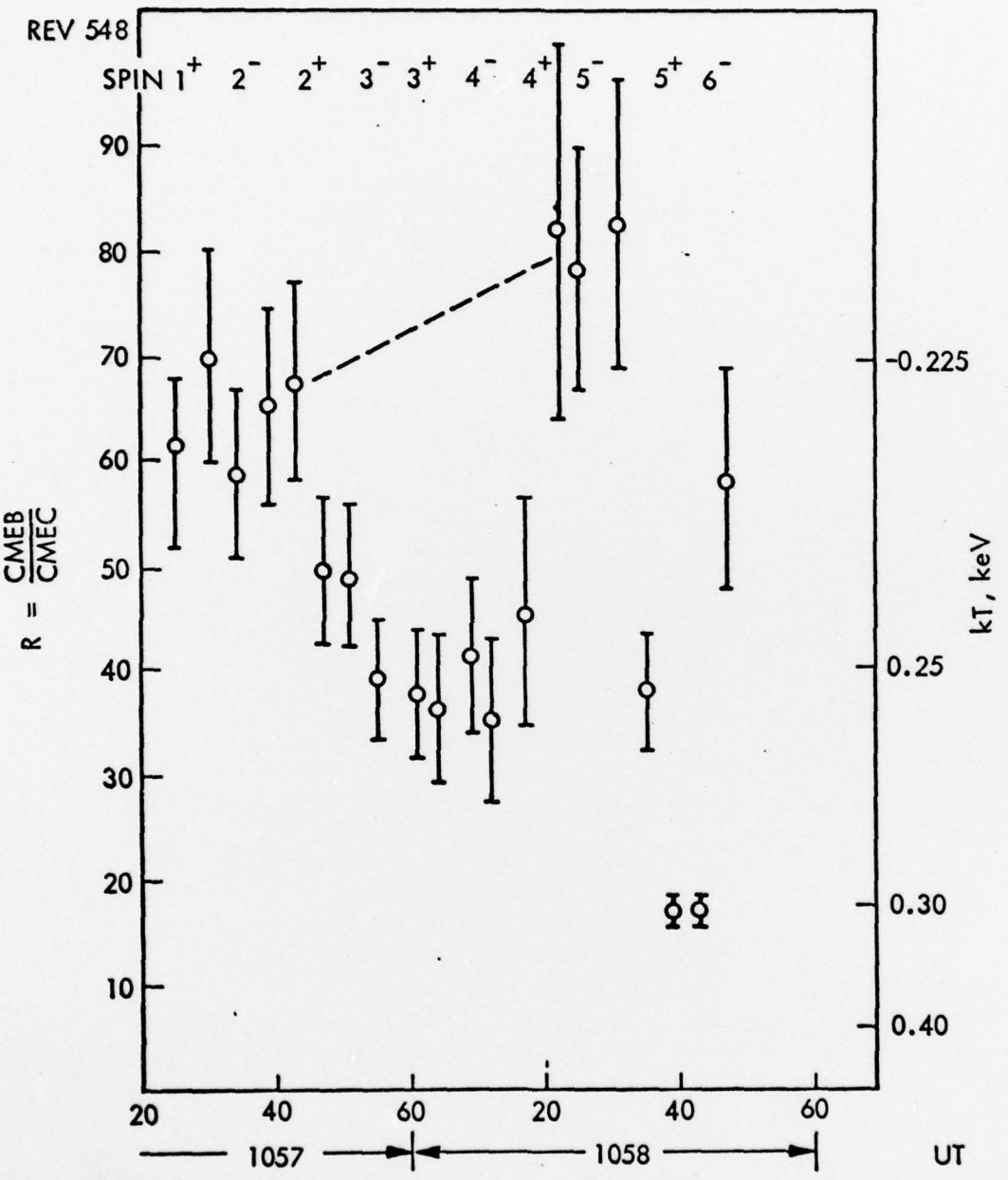
REV 548
SPIN 1+ 2- 2+ 3- 3+ 4- 4+ 5- 5+ 6-
90
80
70
60
50
40
30
20
10
R = CMEB/CMEC
-0.225
0.25
0.30
0.40
kT, keV
20
40
60
20
40
60
1057
1058
UT

Figure 10